**UNIVERSITÀ DEGLI STUDI DI PADOVA**
DIPARTIMENTO DI INGEGNERIA INDUSTRIALE

Corso di Laurea Magistrale in Ingegneria Energetica


**TESI DI LAUREA**

# Wind Farm energy evaluation and modeling from wind data

**Relatore:** **PROF. GIORGIO PAVESI**
**Correlatori** **PROF. RODRIGO GAYA PICOS**

**Laureando:** **MARCO FABRIS**

**ANNO ACCADEMICO 2017-2018**

*Dedicata alla mia famiglia,*
*ai miei amici,*
*all'isola di Mallorca,*
*alla speranza di un futuro migliore*
*basato sulle energie pulite.*

## index

# 1 Introduction

Since ancient times man has used the energy to promote their own well-being and their development. Without the exploitation of energy resources it would not have been possible to reach and build the world and the society that we live today. The massive use of energy resources has become relevant since the Industrial Revolution, when it began to use the first steam engines, were born the first industries and began an increasingly intensive use of fossil fuels. The world we live in today is intrinsically connected in a social, political and economical side with the use of energy. The exploitation of energy resources, especially fossil fuels created new problems worldwide such as pollution, global warming and the greenhouse effect, atmospheric aerosols etc. These reasons are pushing the current policies to a strategic change and preventive use of energy resources which involves a move away from fossil fuels and non-renewable, towards an increasing use of renewable and clean energy resources. Human efforts to harness wind for energy date back to the ancient times for at least 3000 years, when he used sails to propel ships and boats. Later, wind energy served the humankind by energising his grain grinding mills and water pumps. During its transformation from these crude and heavy devices to today's efficient and sophisticated machines, the technology went through various phases of development. The era of wind electric generators began close to 1900's. The first modern wind turbine, specifically designed for electricity generation, was constructed in Denmark in 1890. The oil crisis in 1973, however, forced the scientists, engineers and policy makers to have a second thought on the fossil fuel dependence. They realised that political tampering can restrict the availability and escalate the cost of fossil fuels. Moreover, it was realised that the fossil fuel reserve would be exhausted one day or the other. Wind power, as an concrete and viable alternative to burning fossil fuels to generated electricity, is plentiful, renewable, widely distributed, clean, produces no greenhouse gas emissions during operation, consumes no water, and uses little land. The net are far less problematic than those of nonrenewable power sources. Wind is the world's fastest growing energy source today and it has been retaining this position consecutively for the last six years. In 2017, the European wind power accounted for 55% of all new plants built in the energy sector. They were connected to the electricity grid 15,6 GW wind power, a new power that has helped the EU to cover 11.6% of its needs in 2017 and with a total of 169GW of power currently installed, it has surpassed the coal and nuclear plants and remains second only to natural gas in Europe. The cost of producing electricity from wind energy has become competitive with fossil fuels, in many cases is already more convenient and according to the forecast will be the cheapest in absolute.

# 2 Wind Characteristics

The earth's atmosphere can be modelled as a gigantic heat engine. It extracts energy from one reservoir (the sun) and delivers heat to another reservoir at a lower temperature (space). In the process, work is done on the gases in the atmosphere and upon the earth-atmosphere boundary. There will be regions where the air pressure is temporarily higher or lower than average. This difference in air pressure causes atmospheric gases or wind to flow from the region of higher pressure to that of lower pressure. These regions are typically hundreds of kilometres in diameter. Solar radiation, evaporation of water, cloud cover, and surface roughness all play important roles in determining the conditions of the atmosphere

## 2.1 Meteorology of Wind

The basic driving force of air movement is a difference in air pressure between two regions. This air pressure is described by many physical laws. If we considered air how ideal gas, we can described with Boyle's law(Eq.1), which states that the product of pressure and volume of a gas at a constant temperature must be a constant

$$p_1 V_1 = p_2 V_2 \qquad (1)$$

Another law is Charles' law(Eq.2), which states that, for constant pressure, the volume of a gas varies directly with absolute temperature.

$$\frac{V_1}{T_1} = \frac{V_2}{T_2} \qquad (2)$$

The laws of Charles and Boyle can be combined into the ideal gas law (Eq.3):

$$pV = nRT \qquad (3)$$

In this equation, R is the universal gas constant, T is the temperature in Kelvin, V is the volume of gas in m3, n is the number of kilomoles of gas, and p is the pressure in Pascal (N/m2). At standard conditions (0°C and 1 atm), one kilomole of gas occupies 22.414 m3 and the universal gas constant is 8314.5 J/(kmol K). Within the atmosphere, there will be large regions of alternately high and low pressure. These regions are formed by complex mechanisms, which are still not fully understood. Solar radiation, surface cooling, humidity, and the rotation of the earth all play important roles. From the point of view of wind energy, the most striking characteristic of the wind resource is its variability. The wind is highly variable, in geographically and temporally side. This variability persists over a very wide range of scales, both in space and time. This fact is amplified by the cubic relationship with available energy. On a large scale, space variability shows that there are many different climatic regions in the world, some more interesting than others, with regard to wind energy. These regions vary with latitude, which affects the quantity of insolation. Within a same climatic region, there is a large variety on a small scale, depending on physical geography - the proportion of land and sea, the size of land masses and the presence of mountains or plains for example. The type of vegetation can influence the absorption and reflection of solar radiation, temperature and humidity of the air. More locally, the topography has a great effect on the wind climate. On these time-scales, the predictability of the wind is important for integrating large amounts of wind power into the electricity network, to allow the other generating plant supplying the network to be organized appropriately. On still shorter time-scales of minutes down to seconds or less, wind-speed variations known as

turbulence can have a very significant effect on the design and performance of the individual wind turbines, as well as on the quality of power delivered to the network and its effect on consumers. Van der Hoven (1957) built a record wind speed spectrum in Brookhaven, New York, with light peaks corresponding to the synoptic, diurnal, and turbulent effects of Figure 1. Particularly interesting is the so-called "spectral gap" that occurs between the diurnal and turbulent summits, which show that day and night variations can be treated as very distinct from major turbulence. Ideal wind turbines should follow the wind in all its variations to be able to make the most of the collectable energy, however, for the turbulent regions in the corresponding spectrum within 2 minutes, though high potential is too fast to be exploited by Current machines.

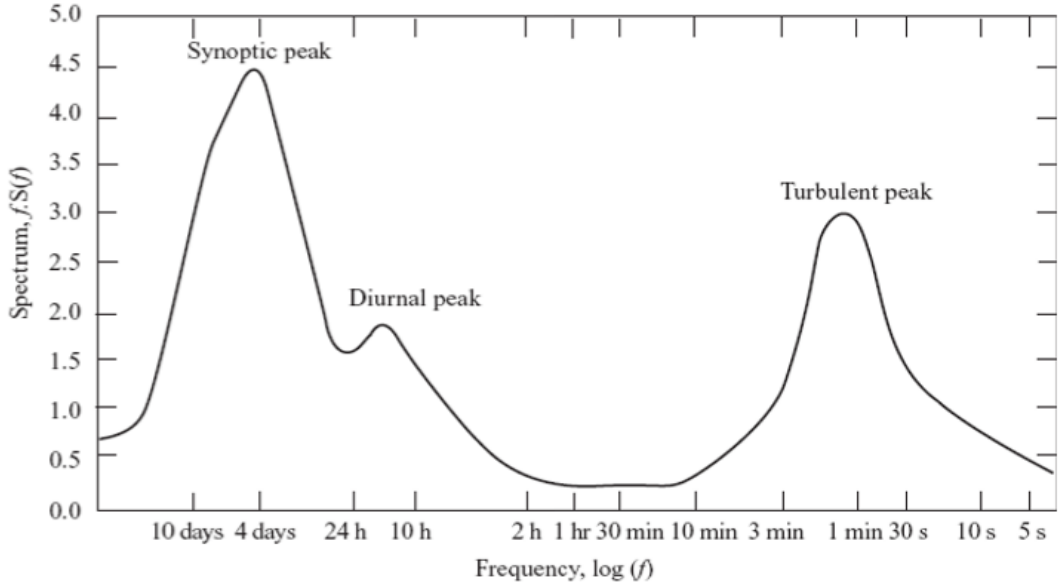


*Figure 1: Wind Spectrum Farm Brookhaven Based on Work by van der Hoven (1957)*

Energy in the form of heat is transferred from the surface of the ground or ocean by evaporation and convection, from the atmosphere to the surface by precipitation, by friction and even in small quantities by conduction. These processes exchange sensitive and latent heat between the atmosphere and the oceans and continents. All movement in the atmosphere is affected by viscosity, therefore the kinetic energy is constantly transformed into heat. So the general circulation must be supported by a renewed energy input.

Air density decreases with temperature rise. Thus, the lighter air of the equator rises into the atmosphere at a certain altitude and then spreads. This causes a pressure drop around this region, which attracts the freshest air from the poles to the equator. The wind that is driven by a temperature gradient, is called geostrophic wind. In Figure 3, global winds, which are not affected by the Earth's surface, are at higher altitudes.

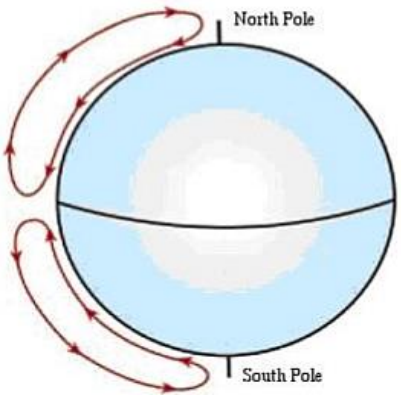


*Figure 3 Geotrophic wind.*

To maintain a high-pressure region while air leaves it at ground level, air must enter the region simultaneously. The only source for this air is above the high pressure region. That is, the air will fall within a high pressure region (and within a low pressure region) to maintain pressure. The descending air will be adiabatically heated and will tend to become dry and clear. Within the low pressure region, rising air is adiabatically cooled, which can cause clouds and precipitation. This is why high pressure regions are usually associated with good weather and low pressure regions with bad weather.

## 2.2 World distribution of the wind

The main winds on the Earth's surface are shown in Figure 5. In some large areas or in some seasons, the actual pattern differs strongly from this idealized image.

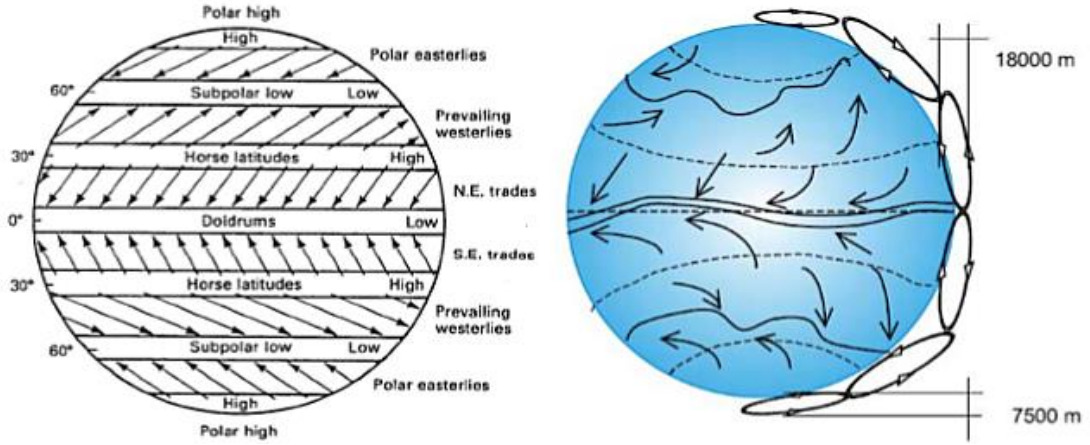


*Figure 5: Terrestrial pressure and wind system*

Combining these high and low pressure areas with Coriolis force produces the prevailing winds shown in Figure 5. The winds of the north-east and southeast winds are among the most constant winds on the ground, at least in the oceans. This causes some islands, such as Hawaii (20 ° N. Latitude) and Puerto Rico (18 ° N. Latitude), to have excellent wind resources. The general circulation flow pattern described above is a model for a smooth spherical surface. In fact, the surface of the earth varies greatly from point to point, These different surfaces affect the air flow due to pressure variations, absorption of solar radiation, and the amount of moisture available. The oceans act like a big heat sink forming waves so the air movement is often coupled with ocean circulation. All of these effects lead to differential pressures that vary both global and local winds, such as monsoons. Also, local heating or local cooling can cause persistent local winds on a seasonal or daily basis such as sea breeze and mountain winds. Smaller atmospheric conditions can be divided into secondary and tertiary circulation

Secondary circulations include the following:

- Hurricanes.
- Monsoon circulation.
- Extratropical cyclones.

Tertiary circulations are small-scale, local circulations characterized by local winds. These include the following:

- Land and sea breezes
- Valley and mountain winds
- Monsoon-like flow (example: flow in California passes)
- Foehn winds (dry high-temperature winds on the downwind side of mountain ranges)
- Thunderstorms
- Tornadoes

## 2.3 Air density

The kinetic energy of a moving body is proportional to its mass. The kinetic energy of the wind therefore depends on the air density. In other words, the more air is heavy and the greater the energy that comes to the turbine. At atmospheric pressure and at a temperature of 15 ° C, the dry air has a mass of 1,225 kg per cubic meter (standard value in the treatment of wind energy when not referring to a specific situation), but the density decreases slightly to ' Increase humidity. In addition, air is denser at lower temperatures, while it is less dense at altitude, due to lower pressure. For dry air the density can be calculated using the ideal gas equation(Eq.4):

$$\rho = \frac{p}{RT} \qquad (4)$$

Where p [Pa] is the pressure, T [K] the absolute temperature and R is the constant of the dry air gas, at R = 287.0 J kg-1 K-1. Alternatively, the relationship to calculate the air density when the temperature and pressure are different from the standard values is obviously the following(Eq.5):

$$\rho = 1{,}225 \frac{228{,}15}{T} \frac{p}{1013{,}3} \qquad (5)$$

Where T [K] is the absolute temperature, and B [mbar] is the barometric pressure.
For eolic wind applications, a standard generic reference in temperate regions (medium latitudes) is the international standard ICAO (International Civil Aviation Organization) atmosphere to calculate an average density value, taking into account both temperature and pressure variation The sea level. The ICAO atmosphere takes the temperature of 15 ° C (288.15 K) and the pressure 101325 Pa at sea level, with an initial vertical heat gradient of -6.5 ° C / (1000 m). According to these assumptions, the density of air (always supposedly dry) with the dimension z s.m.m follows the next approximate relationship (to be used up to z = 2000 m) (Eq.6):

$$\rho\langle z\rangle = 1{,}255 e^{\left[\frac{-z}{10262}\right]} \qquad (6)$$

If you want to take into account even the humidity of the air, the ideal gas equation provides(Eq.7):

$$\rho = \frac{1+x}{R_a + xR_v}\frac{p}{T} \qquad (7)$$

Where x [-] (vapor mass per unit of dry air mass) is the humidity specific for humid air, $R_v$ is the gas constant for water vapor ($R_v$ = 461.5 J kg- 1 K-1)

## 2.4 Wind Speed Variation with Height

The flow of air above the ground is retarded by frictional resistance offered by the earth surface (boundary layer effect). This resistance may be caused by the roughness of the ground itself or due to vegetations, buildings and other structures present over the ground. For example, a typical vertical wind profile at a site is shown in *Figure 8* Theoretically, the velocity of wind right over the ground surface should be zero. Velocity increases with height up to a certain elevation. In the above example, the velocity increases noticeably up to 20 m, above which the surface influence is rather feeble.

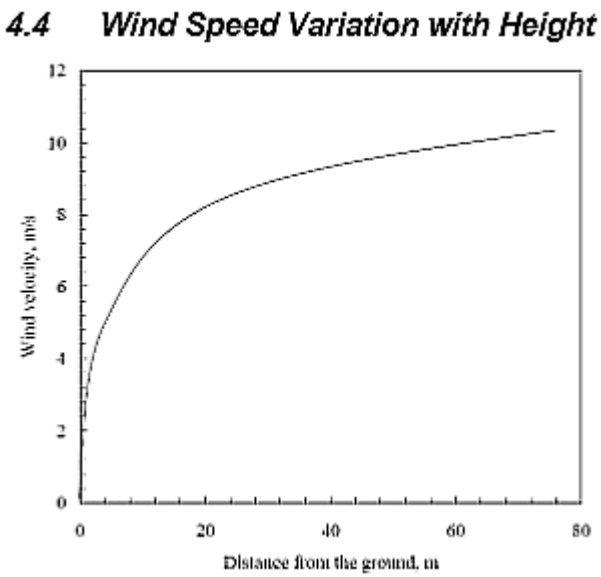


*Figure8: Variation of wind velocity with the height*

The rate at which the velocity increases with height depends on the roughness of the terrain. Presence of dense vegetations like plantations, forests, and bushes slows down the wind considerably. Level and smooth terrains do not have much effect on the wind speed. The surface roughness of a terrain is usually represented by the roughness class or roughness height. Roughness height is an important factor to be considered in the design of wind energy plants. As we see, the wind velocities at these heights are different. Thus, the forces acting on the blades as well as the power available would significantly vary during the rotation of the blades. This effect can be minimized by increasing the tower height. The wind data available at meteorological stations might have been collected from different sensor heights. In most of the cases, the data are logged at 10m as per recommendations of the World Meteorological Organization (WMO). In wind energy calculations, we are concerned with the velocity available at the rotor height. The data collected at any heights can be extrapolated to other heights on the basis of the roughness height of the terrain. The wind velocities at different heights relative to that at 10 m, as affected by the roughness heights, are shown in *Figure 9* In some cases, we may have data from a reference location (meteorological station for example) at a certain height. This data is to be transformed to a different height at another location with similar wind profile but different roughness height (for example, the wind turbine site). Under such situations, it is logical to assume that the wind velocity is not significantly affected by the surface characteristics beyond a certain height. This height may be taken as 60 m from the ground level.

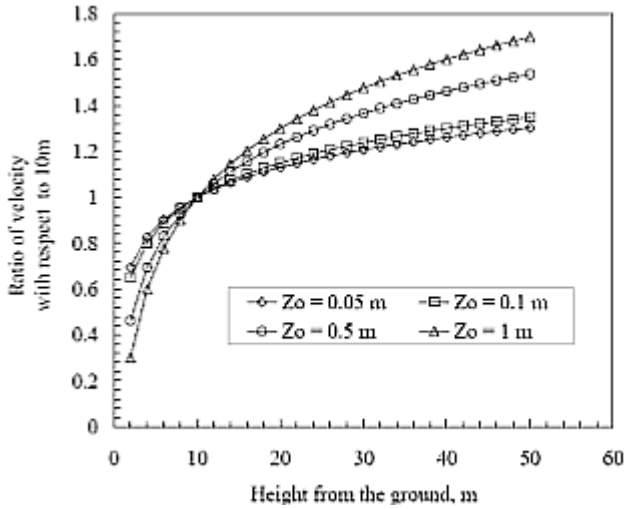


*Figure 9: Velocity ratio with respect to 10 m for different roughness heights*

As we have seen, a knowledge of wind speeds at heights of 20 to 120 m above ground is very desirable in any decision about location and type of wind turbine to be installed. Many times, these data are not available and some estimate must be made from wind speeds measured at about 10 m. This requires an equation which predicts the wind speed at one height in terms of the measured speed at another, lower, height. Such equations are developed in texts on fluid mechanics. The derivations are beyond the scope of this text so we shall just use the results. One possible form for the variation of wind speed u(z) with height z is(Eq.8):

$$u(z) = \frac{u_f}{K}\left[ln\frac{z}{z_0} - \xi\left(\frac{z}{L}\right)\right] \qquad (8)$$

Here $u_f$ is the friction velocity, K is the von Karmans constant (normally assumed to be 0.4), $z_0$ is the surface roughness length, and L is a scale factor called the Monin Obukov length [Panofsky, H. A. (1977), Justus, C. G. (1978)]. The function $\xi\left(\frac{z}{L}\right)$ is determined by the net solar radiation at the site. This equation applies to short term (e.g. 1 minute) average wind speeds, but not to monthly or yearly averages. The surface roughness length $z_0$ will depend on both the size and the spacing of roughness elements such as grass, crops, buildings, etc. Typical values of $z_0$ are about 0.01 cm for water or snow surfaces, 1 cm for short grass, 25 cm for tall grass or crops, and 1 to 4 m for forest and city [Putnam, P.C. (1948)]. In practice, cannot be determined precisely from the appearance of a site but is determined from measurements of the wind. The same is true for the friction velocity uf, which is a function of surface friction and the air density, and $\xi\left(\frac{z}{L}\right)$.The parameters are found by measuring the wind at three heights, as three equations (one for each height), and solving for the three unknowns $u_f$ , $z_0$, and $\xi\left(\frac{z}{L}\right)$. This is not a linear equation so nonlinear analysis must be used. The results must be classified by the direction of the wind and the time of year because $z_0$ varies with the upwind surface roughness and the condition of the vegetation. Results must also be classified by the amount of net radiation so the appropriate functional form of $\xi\left(\frac{z}{L}\right)$ can be used. All of this is quite satisfying for detailed studies on certain critical sites, but is too difficult to use for general engineering studies.

This has led many people to look for simpler expressions which will yield satisfactory results even if they are not theoretically exact. The most common of these simpler expressions is the power law, expressed as(Eq.9):

$$\frac{u\,(z_2)}{u\,(z_1)} = \left(\frac{z_2}{z_1}\right)^{\alpha} \qquad (9)$$

In this equation $z_1$ is usually taken as the height of measurement, approximately 10 m, and $z_2$ is the height at which a wind speed estimate is desired. The parameter α is determined empirically. The equation can be made to fit observed wind data reasonably well over the range of 10 to perhaps 100 or 150 m if there are no sharp boundaries in the flow. The exponent α varies with height, time of day, season of the year, nature of the terrain, wind speeds, and temperature [Golding, E. (1976)]. A number of models have been proposed for the variation of α with these variables [Spera, D. A., and T. R. Richards (1979)]. This figure shows one plot for day and another plot for night, each varying with wind speed according to the equation(Eq.10):

$$\alpha = a - b \log_{10} u(z_1) \qquad (10)$$

The coefficients a and b can be determined by a linear regression program. Typical values of a and b are 0.11 and 0.061 in the daytime and 0.38 and 0.209 at night. Several sets of this figure can be generated at each site if necessary. One figure can be developed for each season of the year, for example. Temperature, wind direction, and height effects can also be accommodated by separate figures. Such figures would be valid at only the site where they were measured. They could be used at other sites with similar terrain with some caution, of course. The average value of α has been determined by many measurements around the world to be about one-seventh. This average value should be used only if site specific data is not available, because of the wide range of values that α can assume.

# 3 General Analisys of wind data

In order to estimate the potential of a site's wind power, a significant amount of data is typically collected that needs to be analyzed and interpreted critically. These data, which may be available for long periods, should be carefully extrapolated to represent the wind profile in the potential site. The minimum period for collecting significant data is typically one year. Modern wind measurement systems provide the average wind speed at the site, averaging at a predetermined time. Usually, data is collected every 10 minutes For example, if we want to estimate available energy for several hours, the data must be grouped by time. Data can also be classified on a daily, monthly or yearly basis.

## 3.1 Average wind speed

Wind speed is generally very variable in intensity and direction, which is why it is usually studied with a statistical approach. Fundamental magnitude is the arithmetic mean. If we have a set of ui numbers, the average of the set is definedas(Eq.11):

$$\bar{u} = \frac{1}{n}\sum_{i=1}^{n} u_i \qquad (11)$$

The size of the sample or the number of measured values is n. However, for wind energy calculations, it is more interesting to study the average wind power and therefore the average speed must be weighed for its power content, or by calculating the average cubic velocity. Therefore, the average velocity of the wind is given by(Eq.12):

$$u_m = \left(\frac{1}{n}\sum_{i=1}^{n} u_i^3\right)^{\frac{1}{3}} \qquad (12)$$

In addition to the average, we are interested in the variability of the set of numbers. We want to find the deviation of each number from the average and then find a kind of average of these deviations. The variance σ2 of data is then defined as(Eq.13):

$$\sigma^2 = \frac{1}{n-1}\sum_{i=1}^{n}(u_i - \bar{u})^2 \qquad (13)$$

Wind speeds are normally measured in full values (intervals). The number of observations of a particular wind speed is defined as $m_i$. The average is then(Eq.14):

$$\bar{u} = \frac{1}{n}\sum_{i=1}^{n} m_i u_i \qquad (14)$$

Now we will define the probability that the discrete wind speed is observed as(Eq.15):

$$p(u_i) = \frac{m_i}{n} \qquad (15)$$

With this definition, the sum of all probabilities will be unity(Eq.16):

$$\sum_{i=1}^{w} p(u_i) = 1 \qquad (16)$$

We define the cumulative distribution function F ($\boldsymbol{u_i}$) (Eq.17) such as the probability that a measured wind velocity is less than or equal to $\boldsymbol{u_i}$.

$$F(u_i) = \sum_{i=1}^{j} p(u_i) \qquad (17)$$

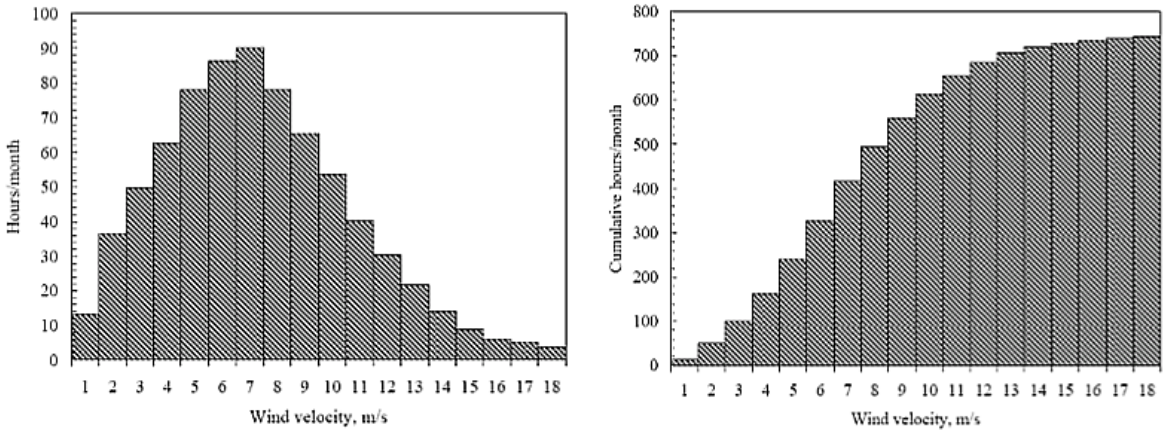


*Figure 10 General relationship between (a) a density function f(u) and (b) a distribution function F(u)*

It may also be helpful to know the probability that wind speeds fall within a range. We call this probability P (ua ≤ u ≤ ub) It is defined as (Eq.18):

$$P(u_a \leq u \leq u_b) = \sum_{i=a}^{b} p(u_i) \qquad (18)$$

It is convenient for a number of theoretical reasons to model the wind frequency curve with a continuous mathematical function rather than a discrete discrete table. Thus, probability values p (ui) become a density function f (u). The area under the density function is the unit, which is shown by the integer (Eq.19):

$$\int_0^{\infty} f(u)du = 1 \qquad (19)$$

The cumulative distribution function $F(U)$ is given by (Eq.1):

$$F(U) = \int_0^u f(x)dx \qquad (20)$$

The x variable inside the integer is just a dummy variable representing the wind speed for integration. Both of the above additions start at zero because wind speed is considered a continuous and positive casual variable (can not be negative) Sometimes we need the reverse of Eq. (20) for calculation purposes. This is given by(Eq.21):

$$f(u) = \frac{dF(u)}{du} \qquad (21)$$

The average value of the density function $f(u)$ is given by (Eq.22):

$$\bar{u} = \int_0^\infty uf(u)du \qquad (22)$$

The variance is given by(Eq.23):

$$\sigma^2 = \int_0^\infty (u - \bar{u})^2 du \qquad (23)$$

These equations are used to compute theoretical values of mean and variance for a wide variety of statistical functions that are used in various applications.

## 3.2 Weibull statistcs

It is logical to represent the wind speed distributions through standard statistical functions. There are several density functions that can be used to describe the wind frequency curve. The two most used are the Weibull and Rayleigh functions. The Weibull is a distribution that depends on two parameters while the Rayleigh has only one parameter. This makes the Weibull a bit more versatile and Rayleigh a bit easier to use. Wind speed follows a Weibull distribution if its probability density function is(Eq.24):

$$f(u) = \frac{k}{c}\left(\frac{u}{c}\right)^{k-1} exp\left[-\left(\frac{u}{c}\right)^{k}\right] \qquad (24)$$

The Weibull distribution depends on two parameters c and k, which are respectively the parameter of the scale and the shape parameter. The curves of $f(u)$ are given in Figure 11 for the scale parameter c = 1. It can be seen that the Weibull density function becomes narrower and higher as k increases. The spike also moves to the right when k increases. Data collected in many locations in the world can be reasonably described by the Weibull density function if the period is not too short.

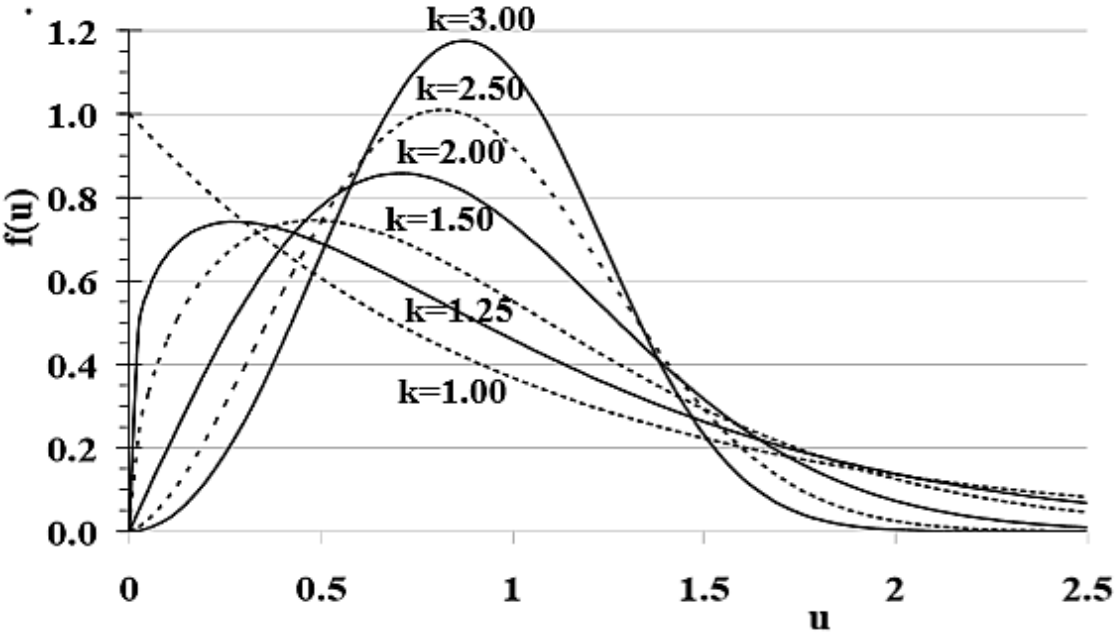


*Figure 11 Weibull density function f(u) for scale parameter c = 1.*

Short periods such as an hour or a day are not generally well-described by a Weibull or any other statistical function, but for longer periods of time than several weeks to a year or more, Weibull generally matches the observed data Reasonably well. If c is different from the unit, the values of the vertical axis must be divided by c, as can be seen from Eq. (40). Because one of the properties of a probability density function is that the area under the curve must be the unit, so when the curve is compressed vertically, it must expand horizontally. For k higher than the unit, f (u) becomes zero at zero wind speeds. The Weibull density function can therefore not adapt a wind speed curve at zero speed. This is not a serious problem for wind power applications because the output of a wind turbine would be zero at a certain cut-in speed. The Weibull density function is a suitable curve for this task.
The average wind speed calculated by also(Eq.25):

$$\bar{u} = \int_0^{\infty} u \frac{k}{c} \left(\frac{u}{c}\right)^{k-1} exp\left[-\left(\frac{u}{c}\right)^{k}\right] du \qquad (25)$$

If we make the change of variable(Eq.26):

$$x = \left(\frac{u}{c}\right)^{k} \qquad (26)$$

then the mean wind speed can be written(Eq.27):

$$\bar{u} = c \int_0^{\infty} x^{\frac{1}{k}} e^{-x} \qquad (27)$$

It is written as a gamma function. The gamma function, $\Gamma(y)$, is usually written in the form (Eq.28):

$$\Gamma(y) = \int_0^{\infty} z^{y-1} e^{-z} \qquad (28)$$

Equations (27) and (28) have the same integrand if y = 1+1/k. Therefore the mean wind speed is(Eq.29):

$$\bar{u} = c\Gamma\left\{1 + \frac{1}{k}\right\} \qquad (29)$$

It may be the most convenient way to calculate gamma function in many situations. Normally, with wind data collected on a site, you directly calculate the average speed. We want to find c and k from the data. For k values below the unit, the ratio c / ū decreases rapidly. For k over 1,5 and less than 3 or 4, the ratio c / ū is essentially a constant, with a value of about 1.12. This means that the scale parameter is directly proportional to the average wind speed fixed to k

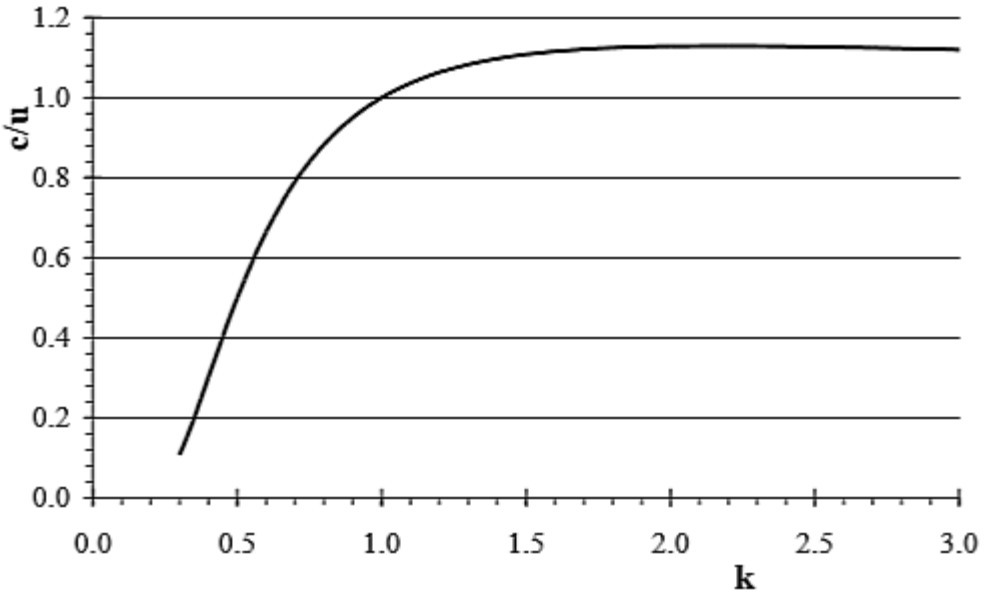


*Figure 12 Weibull scale parameter c divided by mean wind speed u versus Weibull shape parameter k*

It can be shown by substitution that the Weibull distribution function F(u) which satisfies is (Eq.30):

$$F(u) = 1 - exp\left[-\left(\frac{u}{c}\right)^k\right] \qquad (30)$$

The variance of the Weibull density function can be shown to be(Eq.31):

$$\sigma^2 = c^2\left[\Gamma\left(1+\frac{2}{k}\right) - \Gamma^2\left(1+\frac{1}{k}\right)\right] \qquad (31)$$

The probability of the wind speed u being equal to or greater than ua is(Eq.32):

$$P(u \geq u_a) = \int_{u_a}^{\infty} f(u)du = exp\left[-\left(\frac{u}{c}\right)^k\right] \qquad (32)$$

We shall see that the power in the wind passing through an area A perpendicular to the wind is given by (Eq.33):

$$P_w = \frac{1}{2}\rho A u^3 \quad [W] \qquad (33)$$

The average power in the wind is then(Eq.34):

$$\overline{P_w} = \frac{1}{2}\rho A \sum_{i=1}^{w} p(u_i)u_i^3 \ [W] \qquad (34)$$

In fact, wind speeds outside a certain range are unsuitable for a practical wind turbine. Wind speed ume is the speed that produces more energy (the product of power and time) than any

other wind speed. Therefore, the maximum energy obtained from any wind speed is(Eq.35):

$$W_{max} = \frac{1}{2}\rho A u_{me}^3 f(u_m) \quad [W] \qquad (35)$$

Some applications will also require the turbine to be designed with a nominal wind speed equal to this maximum wind speed. This can be found by multiplying Eq. (25) from u ^ 3, setting the derivative equal to zero and solving for u. After a series of algebraic operations, it results(Eq.36):

$$u_{me} = c\left(\frac{k+2}{k}\right)^{\frac{1}{k}} \qquad \left[\frac{m}{s}\right] \qquad (36)$$

Generally, $u_{me}$ is higher than the average speed.

### 3.2.1 Determining the Weibull Parameters

There are several more or less precise methods to determine Weibull c and k parameters. If you know the wind speed average and wind variance, then Eqs. (29) and (31) can be solved directly for c and k. At first glance, this would seem impossible because k is within the scope of a gamma function. However, Justus, C. G. (1978) has determined that an approximation acceptable for k from (Eq. 31) is(Eq.37):

$$k = \left(\frac{\sigma}{\bar{u}}\right)^{-1,036} \qquad (37)$$

This is a reasonably good approximation over the range 1 ≤k≤ 10. Once k has been determined, Eq. (29) can be solved for c(Eq.38):

$$c = \frac{\bar{u}}{\Gamma\left(1+\frac{1}{k}\right)} \qquad (38)$$

More accurately, c can be found using the expression(Eq.39):

$$c = \frac{\bar{u}k^{2,6674}}{0,184 + 0,816^{2,7385}} \qquad (39)$$

Another method of determining c and k which lends itself to computer analysis, is the least squares approximation to a straight line. In the graphical method, we transform the cumulative distribution function in to a linear form, adopting logarithmic scales. That is, we perform the necessary mathematical operations on Eq. (24) to linearize it and then determine c and k to minimize the least squared error between the linearized ideal curve and the actual data points of p(ui). The first step of linearization is to integrate Eq. (21). This yields the distribution function F(u) which is given by Eq. (30). The expression for the cumulative distribution of wind velocity can be rewritten as(Eq.40):

$$1 - F(u) = exp\left[-\left(\frac{u}{c}\right)^{k}\right] \qquad (40)$$

F (u) is more readable than the straight line of f (u), but is still quite nonlinear. F (u) contains an exponential and that, in general, the exponents are linearized by taking the logarithm. In this case, to linearize we have to take logarithms twice (Eq.41):

$$ln\{-ln[1 - F(u)]\} = kln(u) - kln(c) \qquad (41)$$

This is in the form of an equation of a straight line(Eq.42):

$$y = ax + b \qquad (42)$$

where x and y are variables, a is the slope, and b is the intercept of the line on the y axis. In particular(Eq.43) (Eq.44) (Eq.45) (Eq.46):

$$y = ln\left[-ln\left(1 - F(u)\right)\right] \qquad (43)$$
$$a = k \qquad (44)$$
$$x = \ln(u) \qquad (45)$$
$$b = -kln(c) \qquad (46)$$

Data will be expressed in the form of pairs of values of ui and F(ui). For each wind speed ui there is a corresponding value of the cumulative distribution function F(ui). When given values for u = ui and F(u) = F(ui) we can find values for x = xi and y = yi. Being actual data, these pairs of values do not fall exactly on a straight line, of course. The idea is to determine the values of a and b in (Eq. 42) such that a straight line drawn through these points has the best possible fit. It can be shown that the proper values for a and b are (Eq.47), (Eq.48):

$$a = \frac{\sum_{i=1}^{w}(x_i - \bar{x})(y_i - \bar{y})}{\sum_{i=1}^{w}(x_i - \bar{x})^2} \qquad (47)$$

$$b = \bar{y}_l - a\bar{x}_l \qquad (48)$$

In these equations and are the mean values of xi and yi, and w is the total number of pairs of values available. The final results for the Weibull parameters are(Eq.49), (Eq.50):

$$k = a \qquad (49)$$

$$c = exp\left(-\frac{b}{k}\right) \qquad (50)$$

## 3.3 Wind rose

In addition to the statistical distribution of speed, it is useful to have the wind rose of a site (*figure13*). It essentially shows, in polar representation, the statistical distribution of the wind direction of the wind usually in the annual arc. The unique shape of the wind of the figure divides the entire angle into twelve sectors, each of 30 °, but more sector can be used. The three polar representations, all normalized with respect to the maximum value that is

represented by the maximum coordinate of the diagram, provide: a-relative wind frequency in the twelve sectors, That is Say the percentage of total time the wind blows from the direction considered; B- the above figure, multiplied by the average wind speed in the considered direction, and this allows to determine how much each directional sector contributes to the average velocity of the wind; C-the given figure in a- multiplied by the cube of the average cubic wind speed in each sector, and this allows to determine how each directional sector contributes to the total wind energy availability. For example, the wind of a particular site allows you to ascertain the nature of obstacles that may be present in the most favorable directions for energy production, or to plan the location of the various machines on a wind farm. Especially for the location of wind turbines in a wind farm, it is important that machines do not interfere with each other in the direction of maximum wind energy. If the direction of maximum wind power availability is not well-defined within a limited circle of circumference (and its opposite) on a particular site, it is not generally reasonable to construct a wind farm on the site in question.

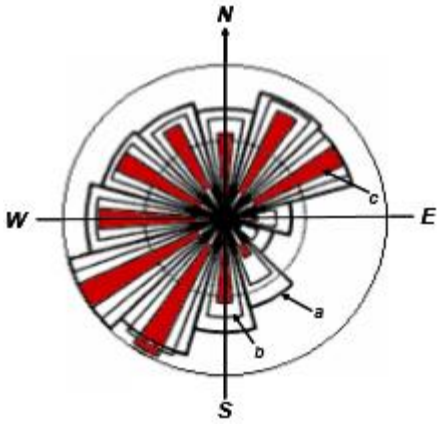


*Figure13: Wind rose*

# 4 Real performance of wind generatos

## 4.1 Betz limit of ideal wind generators

The greater the kinetic energy the turbine manages to extract from the wind and the greater the wind speed that leaves the turbine. The wind is then braked so that the wind speed downstream is between zero and the upstream speed value (for the second of these limit cases the extracted power would naturally be zero). An ideal wind turbine slows down the wind of a factor of 2/3 compared to the upstream speed of the turbine. This figure is the result of the Law of Betz, according to which less than 16/27 (or 59%) of the kinetic energy of wind can be converted into mechanical energy using a wind turbine. Betz's theory does not refer to any specific device for capturing wind power; It will be made in the following reference to an actuator disk, understood as a generic conversion device, which functionally is assimilated to a surface with air flow permeability. The underlying hypotheses of Betz's theory are as follows:

1. The current tube passing through the actuator disc does not interact with the remaining fluid portion surrounding it.
2. In each section of the flow tube there is a permanent, uniform and one-dimensional distribution of axial velocity. Vena slowdown on the actuator disk is evenly distributed on the disk section.
3. In infinitely upstream and downstream sections, a fluid-dynamic situation can be considered undisturbed by the presence of the machine, that is, the atmospheric pressure of the external environment, as in the free casting condition.
4. The wind does not encounter obstacles beyond the turbine, neither overhang nor overflow
5. The wind is stationary and constant intensity with the quota.
6. There are no effects of rotation of the vein due to the "extraction" of the amount of motion.
7. The air compressibility is neglected, that is the density is kept constant.
8. The viscosity effects of the air are neglected.

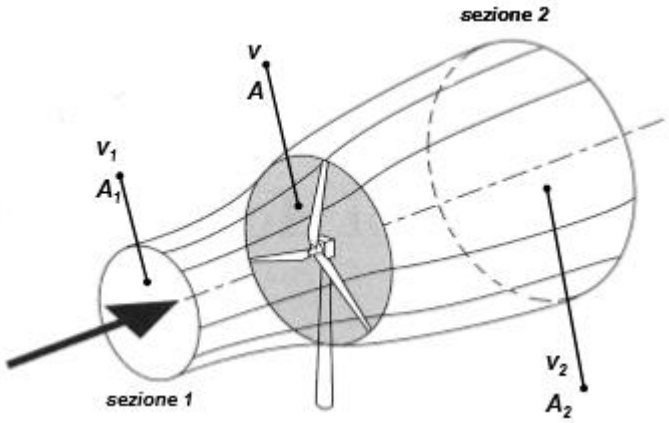


*Figure14: The actuator Disk The fluid vein, characterized upstream (section 1) from undisturbed speed v1, reaches the rotor blades and is slowed down to a speed v2 in section 2.*

Of course, in the passage 1 to 2, the continuity equation must be valid, so it can be written

(assuming constant density for hypothesis 7) (Eq.51):

$$\rho v_1 A_1 = \rho v_2 A_2 = \dot{m} \qquad (51)$$

The equation of the amount of motion must also be verified for which(Eq.52):

$$T = \dot{m}(v_1 - v_2) \qquad (52)$$

T is the force (horizontal) exerted by the flow on the machine (referred to as the temporal mean of force in the course of a complete revolution of the rotor).
The power is therefore(Eq.53):

$$P = Tv = v\dot{m}(v_1 - v_2) \qquad (53)$$

By making a balance between the entry and exit of the kinetic energy associated with the fluid vein there is the power sold(Eq.54):

$$P = \dot{m}\frac{v_1^2 - v_2^2}{2} \qquad (54)$$

But since the powers found in the two modes have to coincide, is obtained, *v=(v1+v2)/2* so that the slowdown occurs halfway in the upstream and midway section of the downstream current section of the actuator disk. The axial interference factor such as(Eq.55):

$$a = 1 - \frac{v}{v_1} = \frac{v_1 - v}{v_1} \qquad (55)$$

We get v = v1 (1 - a), but since v = (v1 + v2) / 2 we have v2 = v1 (1-2a). The factor a represents the extent to which the flow is slowed upstream of the turbine (at the limit of a = 0.5 when the flow block is in the output section 2). By substituting the relationships found for velocities v and v2 in the expression of power (53) we obtain the power that can be extracted from a wind stream according to Betz theory(Eq.56):

$$P = \frac{1}{2}A\rho v_1^3 4a(1-a)^2 \qquad (56)$$

By imposing the deletion of the derivative before P with respect to, the optimal interference can be found (the interference for which the maximum power is extracted):
A = 1 or a = 1/3. The value a = 1 does not make sense for it to = 1/3.
A $C_P$ power coefficient can be defined as the relationship between power P and power P0 evaluated in the undisturbed fluid vein(Eq.57), (Eq.58):

$$P_0 = \frac{1}{2}\rho A v_1^3 \qquad (57)$$

$$C_p = \frac{P}{P_0} = 4a(1-a)^2 \qquad (58)$$

The value of the power coefficient for a = 1/3 is Cp max = 16/27≈0.59. It can therefore be subtracted to Up to 59% of the power associated with the fluid vein. (Note that the power coefficient defined here is sometimes referred to as "rotor, CPR", as it refers to the rotor powerable power, regardless of the mechanical and electrical leaks always present in a wind turbine). This result can also be seen graphically in Figure15. In fact, the power coefficient can be written according to the speed ratio v2 / v1(Eq.59):

$$\frac{P}{P_0} = \left(\frac{1}{2}\right)\left(1 - \frac{v_2}{v_1}\right)\left(1 + \frac{v_2}{v_1}\right)^2 \qquad (59)$$

This function is shown in *Figure 15* and, as we see it, has its maximum for v2 / v1 = 1/3 and the maximum of the extractable power is about 59% of the total wind power.

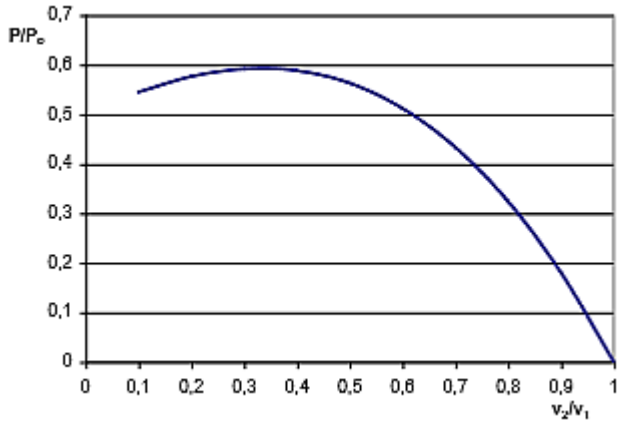


*Figure15: Rapresenting of maximun power extractable for Betz theory*

Finally, the force that tends to reverse the machine (axial thrust) is(Eq.60):

$$T = \frac{1}{2}\rho A v_1^2 4a(1-a) \qquad (60)$$

Defining the CT thrust coefficient and torque coefficient CM as follows(Eq.61), (Eq.62):

$$C_T = \frac{T}{\frac{1}{2}\rho A v_1^2} \qquad (61)$$

$$C_M = \frac{M_r}{\frac{1}{2}\rho A v_1^2 R} \qquad (62)$$

Where Mr = drive torque of the actuator disk, Mr=P/ω (ω is the rotation speed of the radius of the radius of the R radius), it has(Eq.63), (Eq.64):

$$C_T = 4a(1-a) \qquad (63)$$

$$C_M = \frac{C_p}{\lambda} = \frac{4a(1-a)^2}{\lambda} \qquad (64)$$

Where λ is the ratio between the peripheral speed of the rotating actuator disk and undisturbed wind speed v1, Is called a Tip speed ratio(Eq.65):

$$\lambda = \frac{U}{v_1} = \frac{\omega R}{v_1} \qquad (65)$$

It should be explicitly observed that Betz's axial impulsive theory does not make any reference to the type of machine that extract energy from the wind flow tube (it is a general actuator disk) and does not assume any dissipative phenomenon with respect to ' Energy originally contained in the fluid current (the flow is supposed to be non-viscous). In fact, the maximum value less than one of the power coefficient derives from referring to the power obtained at the own power value of the air flow passing through an area equal to that affected by the actuator disk at undisturbed wind speed. Actually, through the actuator disc passes a lower air flow (due to the slowdown of the fluid current upstream the actuator disk), the lower the fluid flow slows down. The power is obtained by the product of the air flow through the section of the actuator disk multiplied by the variation of the specific kinetic energy between the mountain and the valley; At decreasing speed v2 downstream, increases the kinetic energy variation, but decreases the utilized air flow: the maximum power value is in the compromise condition between these two contrasting actions, and is obtained when the downstream velocity v2 Is reduced to one third of the value of the upstream speed v1. As an example, consider the limit case, with the full exploitation of the total kinetic energy of the wind; In this case it would result in the limit v2 = 0 and the limit state of the infinite area for the flow tube downstream of the wind generator. In this condition is for the wind speed at the actuator disk v = v1 / 2, and consequently the power actually exploitable is half the reference power, and then CP = 0.5 as the limit is from the expression (58). *Figure 16* illustrates the evolution of the various characteristic quantities along the flow tube, in the hypotheses of Betz's theory and in the state of maximum power extracted. At a distance from the rotor it is shown that the wind speed equals the undisturbed value v1 as a result of the movement of the amount of motion with the surrounding air mass: the invisible motion hypothesis is apparently released downstream of section 2.

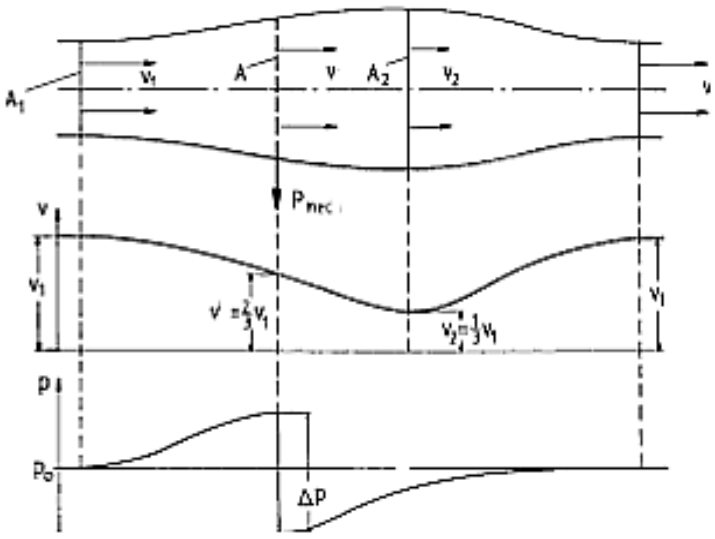


*figure16: Velocity and pressure variation of Betz theory*

## 4.2 Real performance of wind rotor

It has already been noted that Betz's theory comes to fix a limit on the fraction of the total power present in a suction current by a wind rotor, without considering any dissipative process or energy loss. This is due to the fact that a wind turbine in operation can not interfere with the total air flow which, if undisturbed, would cross an area equivalent to that of the actuating disk due to the required expansion of the flow tube section upstream of the rotor. Betz impulsive axial theory, referring to a generic air flow-permeable actuator disk as a power capture device, assumes an air velocity velocity downstream of the axial turbine, and calculates the kinetic energy variation between Mount and valley of the actuator disk accordingly. The air flow is slow and the flow lines are deflected only in one plane. While always remaining in the ideal no-viscosity flow, without dissipative phenomena, and specifically referring to a rotating rotor with a horizontal rotation axis, it is necessary to consider that a rotating converter necessarily gives a rotating motion To the stream of air; To maintain the amount of tangential motion the helical motion of the air stream will have a rotational direction opposite to that of the rotor itself: see *Figure 17* The existence of a velocity tangential component obviously reduces the variation of kinetic energy induced by the rotor than calculated by the theory of Betz. As a result, the rotor power coefficient is reduced, depending on the relationship between the rotating motor energy component and that of axial translation motion.

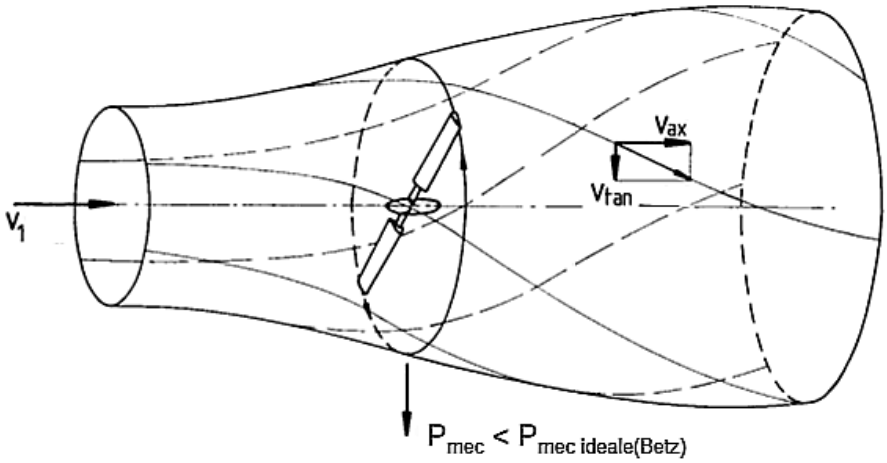


*Figure17: Tangential and axial componente of velocity*

This ratio, calculated globally over the entire length of a shovel, is directly related to the already encountered Tip speed ratio parameter is the speed of the end of the blade, radius R [m] and rotating at angular velocity ω [rad s-1]. It is common practice to speak of rotational speed of the $N_g$ rotor in terms of RPM <rpm> in the literature Anglo-Saxon. In that case it is obvious for these equations (Eq.66), (Eq.67), (Eq.68):

$$U = \frac{2\pi R N_g}{60} \qquad (66)$$

$$\omega = \frac{2\pi N_g}{60} \qquad (67)$$

$$\lambda = \frac{2\pi R N_g}{60} \qquad (68)$$

The tip speed ratio is the aerodynamic similarity parameter for geometrically similar rotors. The problem can be treated analytically with the swirling impulse theory applied to the ideal invisibility situation. One should consider (*figure 18*) individual shovel elements, evaluating them aerodynamic actions in relation to local physical conditions, and integrating effects on the entire length of the blades (Theory of the blade elements).

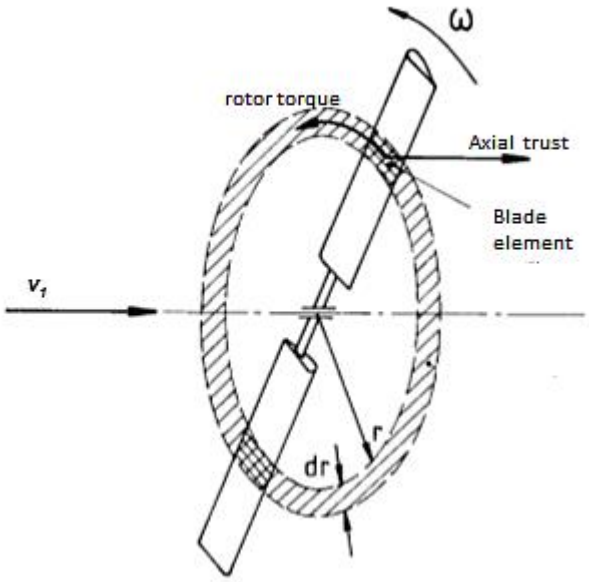


*Figure18: aerodynamic actions in local element of blades*

This theory shows that in optimized conditions (maximum power) the trend of the CPR rotor power coefficient according to the peripheral velocity ratio λ is that shown in *Figure18* from the curve immediately below the value (constant λ) of the ideal power coefficient of Betz, and that deviates from this for wake losses. At low tip speed ratios, even under optimally optimized conditions, the kinetic energy loss due to the spin speed may be elevated; Only to the λ tendency to infinity, such losses tend to be canceled (decreasing the flow rotation) and the power coefficient tends to the ideal value of Betz.

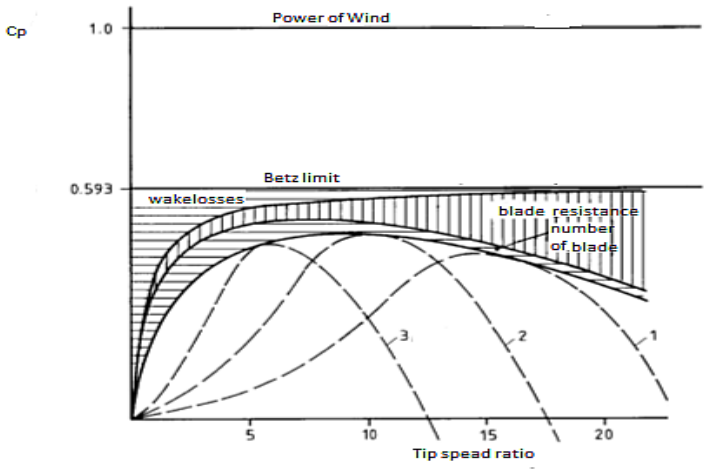


*Figure19: Cp in real wind turbines with losses*

It has been said that in almost all cases for modern wind turbines the blades have a wing profile; Such is the profile of the blade element (of a small longitudinal dimension with respect to the transverse dimensions, so that the fluodynamic parameters considered are considered constant) shown in *Figure 19*, which rotates at angular velocity ω around the radial distance rotor axis (Media) r. The local wind speed v vectors are represented at the profile edge of the contour and the opposite is the rotational motion vector of the profile element, -rω. The composition of these two vectors allows to obtain the wind speed relative to the blade element, vr. Be careful that v is not the undisturbed wind speed, but the local speed in axial direction. The wind exerts the total force F on the blade element considered, resulting in D (Drag) resistance, component in the direction of relative velocity of the wind vr, and of the bearing L (Lift), which is orthogonal to that of the relative velocity of the Wind vr. By smacking the total force F in the orthogonal direction to the plane of rotation of the blade, the axial thrust T is obtained, while the normal component to this (tangential thrust S) acts in the direction of the rotational speed of the rω profile and provides a useful torque for capturing the wind energy.

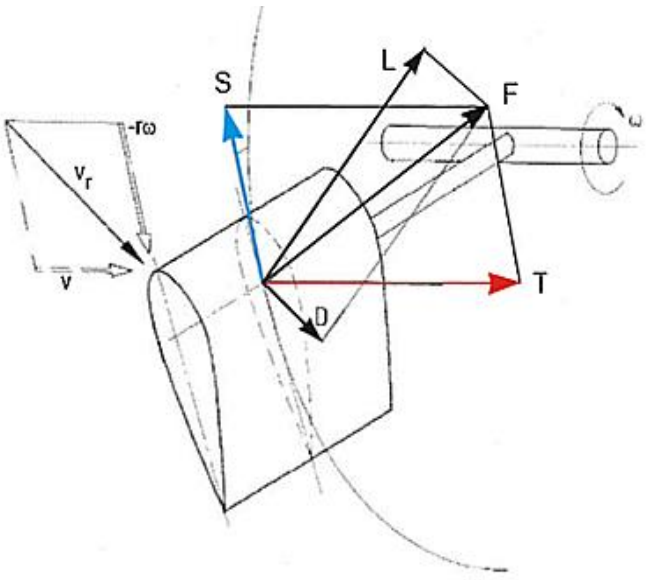


*Figure20: components of the total force in a blade element*

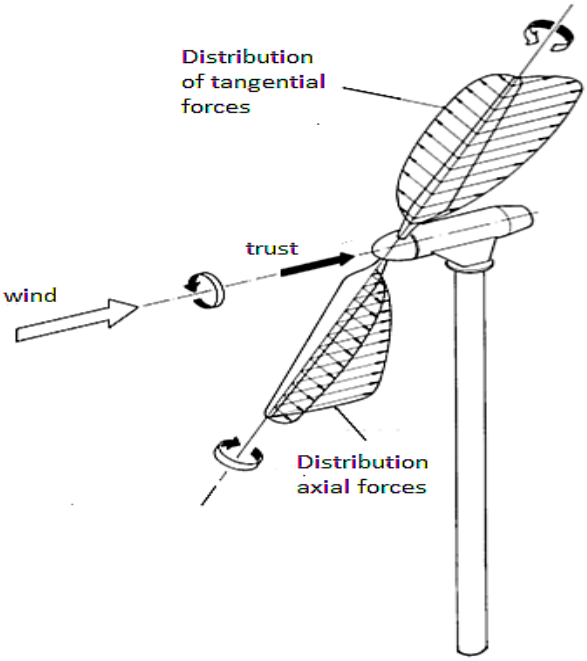


*Figure21: distribution of axial and tangential forces on a bipolar horizontal axis wind turbine.*

It is necessary to examine more in detail the aerodynamic action exerted by a fluid current on a wing profile. As shown in *Figure 22*, the dynamic force profile effect results from an asymmetric distribution of pressures on the opposing faces of the wing profile. The total force F, as mentioned, is used to break in the two components, D Drug and Lift L; The resistance D always agrees with that of the relative wind speed vr. The profile rope is the connecting edge of attack with the output edge; Its length is indicated by c. The angle α that the contour rope forms with the relative direction of the wind is called the angle of attack (or incidence)

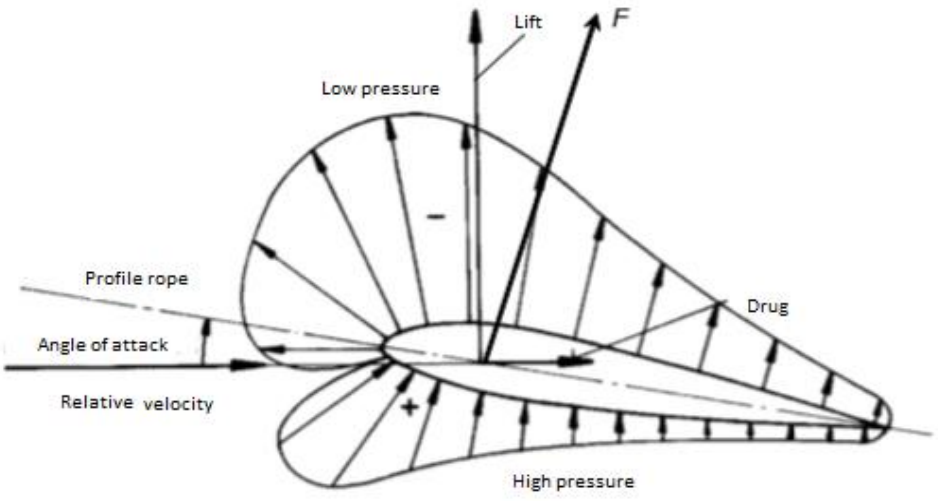


*Figure22: distribution of pressure and force of the profile*

For the profiles, the $C_D$ drug coefficient and the lift coefficient $C_L$ are defined as follows (Eq.69), (Eq.70):

$$C_D = \frac{D}{\frac{1}{2} A_p \rho v_r^2} \qquad (69)$$

$$C_L = \frac{L}{\frac{1}{2} A_p \rho v_r^2} \qquad (70)$$

Where $A_p$ is the profile area, calculated as the product of the length of the rope c for the longitudinal width of the profile considered (normal to the plane of the drawing in *Figure 21*), ρ the air density and vr the air velocity profile.
For geometrically similar aerodynamic profiles, the resistance and drag coefficients depend on the number of Reynolds and vary with the angle of attack α. In wind turbine's own motion regimes, the dependence of aerodynamic coefficients on air compressibility (dipendece of Mach number) can be neglected. The following *figure 23* illustrates the variation of the aerodynamic coefficients $C_D$ and $C_L$ at the variation of the α angle of attack for a defined aerodynamic profile and particular number of Reynolds in the field of wind turbine. In the typical field of application, the lift coefficient $C_L$ increases as the attack angle increases to a characteristic value (critical angle or stall) to which it reaches the maximum value, then more or less abruptly decreases and the coefficient of Drug $C_D$ rises drastically. It is said that the profile operating in stall condition, that is, the manifestation of separation of the fluid threads (vein detachment, with vortex formation) in the down side of the profile.

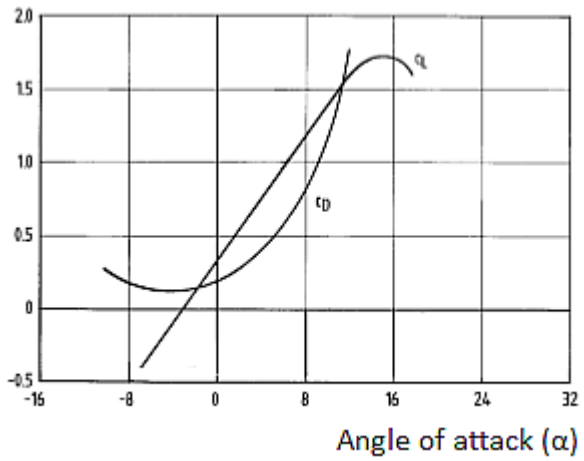


*Figure23: variation of aereodinamic coefficient with the angle of attack*

The following *figure 23* illustrates the trend of the coefficient of drug $C_D$ ras a function of the coefficient of lift $C_L$. Relationship between the values of the lift coefficient and the drug coefficient (Eq.71):

$$E = \frac{L}{D} = \frac{C_L}{C_D} \qquad (71)$$

Is called profile efficiency. In the diagram of *Figure 24*, the maximum value of the profile

efficiency is at an attack angle above 0 °, with a profile efficiency exceeding 200; Represents the optimal working condition of the profile. The maximum efficiency value therefore determines the aerodynamic profile.

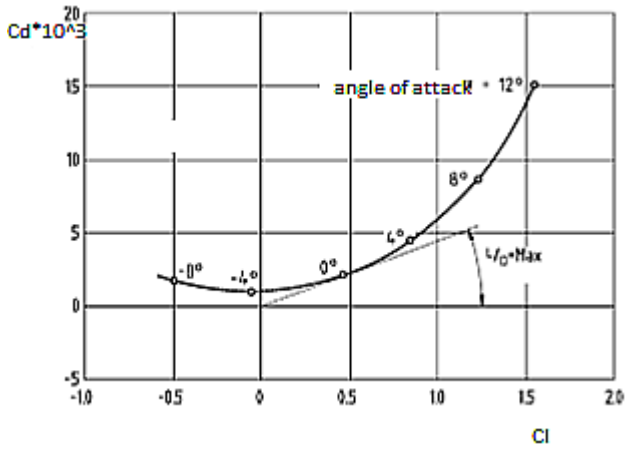


*Figure24: profile efficiency*

Regarding the dependence of the value of the aerodynamic coefficients on the number of Reynolds (and hence the magnitude of the inertia forces relative to the viscous ones) the coefficient of $C_D$ decreases as the number of Reynolds increases, and this increase is drastically below the critical value of Re, when the boundary layer becomes totally laminar. The effect of King on the lift capacity $C_L$ instead manifests itself above all on the value of the stall angle, which increases with the growth of Re; and since the lift coefficient varies linearly with the angle of attack for values below the stall angle, even the maximum lift capacity coefficient increases as the number of Reynolds increases. Moreover, coefficients depend on surface quality; In particular the resistance coefficient increases with the surface roughness. The figure in *figure 25* (assuming v ≈ ⅔ v1 refers to the optimum condition according to Betz) fully summarizes all the force components acting on a shovel element of a HAWT wind turbine. Note that the tangential thrust that produces a useful pair results from the bearing of the profile; On the other hand, the profile resistance always acts in a negative direction on the useful tangential thrust, opposing the useful component of the bearing.

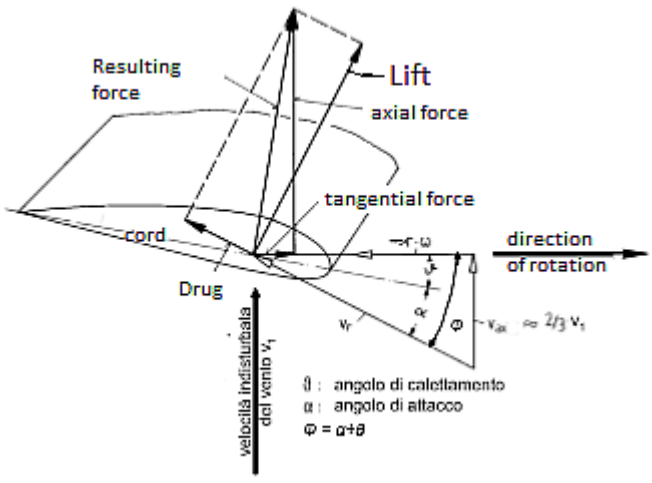


*Figure 25: all the force components acting on a shovel element*

In the same figure, next to the angle of attachment α, the angle θ of the shutter element is highlighted, which is the angle formed between the profile rope and the pivot rotation plane (constructive angle of the shovel). The local value of the hinge angle depends on the blade geometry and the attachment of blade to the hub. Defining the flow angle as(Eq.72):

$$\phi = \alpha + \theta \qquad (72)$$

the sum (angular) angle of the coupling angle and the hinge angle can be obtained by the tangential thrust S and the local axial thrust T on the blade element(Eq.73),(Eq.74):

$$S = L\sin\phi - D\cos\phi \qquad (73)$$

$$T = L\sin\phi + D\cos\phi \qquad (74)$$

So it is also possible to define the tangential thrust coefficient CS and the axial thrust coefficient CT as follows(Eq.75), (Eq.76):

$$C_s = C_L\sin\phi - C_D\cos\phi \qquad (75)$$

$$C_T = C_D\sin\phi + C_L\cos\phi \qquad (76)$$

Which allow to obtain the axial thrust, the tangential thrust and the useful torque produced by the latter in the direction of the rotor motion as follows(Eq.77), (Eq.78), (Eq.79):

$$S = \frac{1}{2}C_S\rho A_P v_r^2 \qquad (77)$$

$$T = \frac{1}{2}C_T\rho A_P v_r^2 \qquad (78)$$

$$M_r = Sr = \frac{1}{2}C_S\rho A_P v_r^2 r \qquad (79)$$

In many modern wind turbines, the angle of fixing the blades on the hub can be continuously varied in motion by rotation of the blades around their longitudinal axis, thereby varying the local bevel angle and consequently the angle of attack, In order to optimize operating conditions, or to limit the power captured above the nominal wind speed, or to place the blades in the flag. As shown in *Figure 26* the local tangential speed of the blade u = ωr varies obviously from the base to the end of the blade. Considering uniformly the component v of the axial velocity of the wind at the edge of the entire blade, varies accordingly the relative velocity vr, not only in magnitude but also in direction. In order to maintain a local value of the angle of attack of good aerodynamic efficiency (constant or little variable), it is necessary to construct the shovel in a saggling manner: the local kinking angle must decrease from base to end of shovel. As also shown in *Figure 26*, for reasons not only structural, the rope of the paving profile generally decreases from base to end. Even the profile of the palisade section may be different to the base of the pallet where structural considerations prevail, also because the power contribution in this area is lower than that of the outer areas (smaller area sweep per unit of length, less relative speed of the

wind, as shown in the same figure). It is to be noted that the locally necessary grinding, for example, to maintain the angle of attack α along the entire blade constant, depends on the value of the relationship between the peripheral speed of the blade and the local wind speed v: geometry optimization of the blade therefore concerns the nominal working conditions. In other operating conditions, shaving of the blade is not optimized, and this inevitably creates efficiency losses.

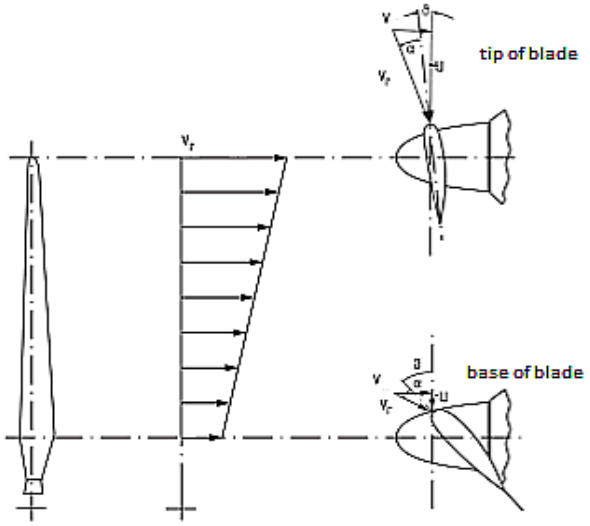


*Figure26: local tangential speed frome the base to the end*

The previous *figure 18* showed the ideal energy performance values (condensed in the rotor power coefficient parameter) as a result of axial impulse (Betz) theory and swirling impulse theory; Both of these theories are based on invisible motion, without viscous action, and therefore without dissipative phenomena. These theories express the inability of the wind rotor to capture the entire power available in the suction current. The non-captured power remains, however, in the gaseous current downstream of the capture device. In particular, the swirling impulse theory (whose optimized results are shown in *Figure 18* from the curve that deduces the power loss of Betz from the wake of leakage) shows how the Cpr rotor power coefficient depends on the value of the peripheral velocity ratio λ. The leakage losses decrease rapidly as the λ increases, tending to be canceled by $\lambda \rightarrow \infty$. The reason for this trend is easily explained by qualitatively. For a specified undisturbed wind speed, the power recovered from each rotor blade is expressed as the product of the useful torque on the blade for the rotation speed of the blade. As the latter increases (and therefore increases the peripheral velocity ratio λ), a smaller torque (and hence a smaller tangential thrust) is required to derive the same power. A lower tangential thrust corresponds to a lower tangential velocity value imprinted at the air flow, and hence a lower skid loss. Swirling impulse theory assumes complete absence of resilient action by the palette, and hence the use of an ideal palisade profile for which it is found for the $L / D \rightarrow \infty$ resistance / resistance ratio. The action of resistance (which results from variation of wind most movement motion in the interference with the blade) manifests, in the drive actuators, by the generation of a torque contrary to the useful rotary motion, and thus to reduce the wind power captured by rotor has already discussed. In addition, impulse theories take into account a generic actuator disk, based on the results across the whole power through that device. In fact, the ability to capture a fraction more or less of this power also depends, for a wind turbine, by

the number and shape of the blades as well as by their rotational speed. Impulse theories therefore consider, in every circumstance, a number of blades, idealized behavior, $\lambda \rightarrow \infty$. Theories that try to interpret the dissipative effects due to the final number of blades to their aerodynamic resistance in terms of penalizing the energy capture efficiency of the various types of wind turbines are complex and transcend the purpose of this discussion. The approach is still to examine aerodynamic actions on shovel elements, and to integrate the effect on the entire length of shovel (see *Figure18*). As to the effect of the number of blades, among the numerous proposed theories, Prandtl's collection pays particular credit for agreement with the experimental data. In summary, the results of the effect of the blade resistance and the finite number of blades on the rotor power coefficient are shown in *Figure 25* always depending on the peripheral velocity ratio λ. It can be seen that the penalty in the power coefficient is consistently decreasing as the number of blades increases and also decreases as the peripheral speed increases. Even this latter effect is easily perceived as, with the same wind speed, a finite number of blades can interact more fully with the entire air flow through the surface swept by the rotor, the greater the Rotation speed of the latter. As to the damaging effect of the palate resistance, it is obvious that this obviously depends on the efficiency (relationship / strength) of the palate profile: at the decrease in the bearing / resistance ratio (L / D), the value of the coefficient of power Achieved diminishes. Alari profiles, under design conditions, work around 50-100 effective values, while curved slab profiles work under optimal conditions around the 10 to 15 efficiency values. It can be generally stated that the optimum point of the power coefficient moves to lesser values of λ when the efficiency of the shaded profile decreases. At high L / D values (≈100), the optimum value of the peripheral speed ratio λ is high, and the number of rotor blades is of little importance in the value of the achievable power coefficient. When, on the other hand, the efficiency of the palisade profile is low (L / D ≈ 10), the values obtained for the power coefficient are considerably lower, obtainable at low values of the peripheral velocity ratio λ, and the number of blades assumes great importance. High speed rotors can have excellent performance with limited number of blades, but the palette profile is of great importance in this case.

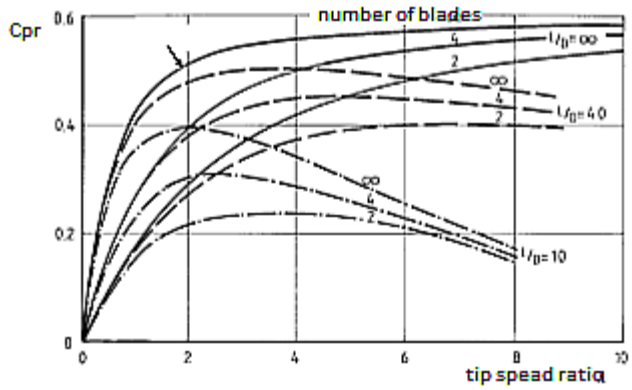


*Figure27: relation of Cp, tip speed ratio and number of blades*

*Figure 27* illustrates, in sufficient indicative terms, the optimum operating ranges of the various types of wind turbines, both HAWT and VAWT, and approximately the values of the rotor power coefficient which under optimum conditions can be expected to be obtained. The superiority of modern HAWT aerodynamic blade rotors, which operate at high peripheral tangential speed values, is superior to traditional rotor (Dutch, American) old lenses (in terms of value of parameter λ). With the latter, it is difficult to achieve, under optimized operating conditions, values of the rotor power coefficient of 0.3, while modern

machines can reach values around 0.5, and therefore not too far from Betz's ideal limit. Number of rotor blades. It has already been seen how, in an intuitive way, the smaller the number of rotor blades, the faster it is (alongside other conditions) to rotate to compensate for the disadvantage of a smaller coverage of the physical disk space actuator. Figure27 shows, the influence of the number of blades on the rotor power coefficient for modern aerogenerators under otherwise optimized conditions; In particular, the figure curves represent the envelope of the characteristic curves of the power coefficients of modern rotors at the variation of the step of the blades. As shown in Figure 27 (specifically referring to the triple WKA-60 rotor), the CPR-λ curve depends on the sloping angle of the blade; Modern rotors with variable blades in motion can in theory adjust the angle of bend optimizing it in the different operating conditions (hence at different values of the peripheral velocity ratio λ), while the blades rotating blades must operate along a single curve characteristic CPR – λ. As can be seen from *Figure 28*, the different types of wind turbines show optimal operation around different values of the peripheral velocity ratio λ: while the multipole American rotors have optimum operation around λ = 1, the single-pole fast rotors operate effectively in A wider range of λ, around the value λ = 15. Different types of machine are characterized by different values of the solidity parameter σ, defined for HAWT rotors as the ratio between the frontal area of the rotor blades (expressed as each blade as a product between the average length of the rope and the longitudinal length Of the shovel Z) and the total area swept by the rotor in its rotary motion.

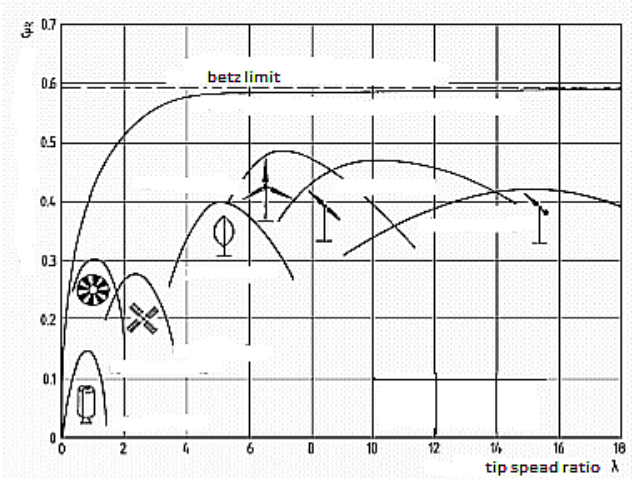


*figure28 relation of Cp, tip speed ratio and type of wind turbine*

In formula (Eq.80):

$$\sigma = \frac{B\bar{c}Z}{\pi R^2} \qquad (80)$$

Since B is the number of rotor blades.

The main effects of rotor strength on wind energy efficiency can be summarized as follows:

- Low strength value produces a wide and fairly flat CPR - λ curve; This means that CPR changes little on a wide range of values of peripheral velocity ratio, but the maximum CPR is low due to the high loss profile for the palate profile.
- A high solidity value produces a narrow CPR - λ curve with a pronounced peak, making the rotor performance very sensitive to changes in the peripheral velocity

ratio; If the solidity value is too high, the maximum CPR value is low, due to leakage losses on the wake.

- A good value (even economical) aspect of solidity is achieved with three-blade HAWT wind turbines (typical values around 0.035), but the two-blade solution can be an acceptable alternative as, although Produces a slightly lower CPR value, the CPR - λ curve is flat, and this can be an advantage over global energy production, especially for machines running at constant rotation speeds.

Alongside the power characteristic, another important operational magnitude of wind turbines is the torque characteristic, also defined by the aforementioned torque coefficient Cm(Eq.81):

$$C_M = \frac{M_r}{\frac{\rho}{2} v_1^2 AR} = \frac{C_P}{\lambda} \qquad (81)$$

*Figure (29)* shows the typical trend of the torque coefficient according to the peripheral speed ratio (for fixed winding blades) for HAWT wind turbine types already considered

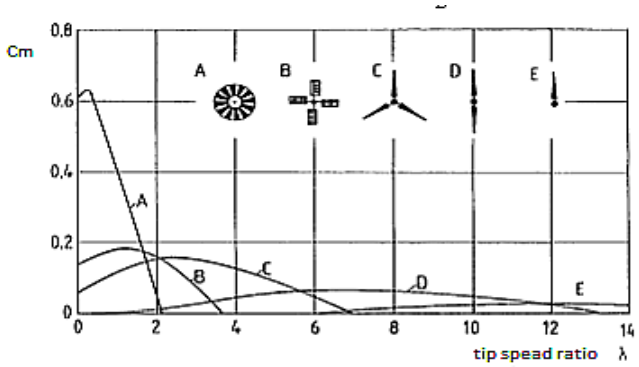


*Figure29: Cm for differents type of wind turbine*

above. The difference between slow multipole rotors and fast ones with low number of blades is evident; In particular, at the start (λ = 0), the first can produce high torque even at modest wind speeds, unlike the seconds. It is easy to understand the inability of the rotor with a limited number of blades to produce a high starting torque: from stops can interact only very limited with the total flow of wind passing through the motorcycle sweep area. Hence the suitability of multipole rotors to operate as aero-motors, for example with the rotor directly connected by mechanical water-pump volumetric pumps (as for classical multiplying American aeromotors) or connected to mills (Dutch windmills). For wind turbines (rotors for power generation), apart from the need for a minimum wind speed to operate (cut-in speed), the low torque value is an advantage for dimensioning the possible multiplier of Speeds between the slow rotor shaft and the fastener of the electric generator.

## 4.3 Power generation of wind turbine

The proper way to evaluate the economic performance of a wind turbine is to consider its energy yield (eg on an annual basis), depending on its power characteristics and a particular wind regimen. For a certain diameter of the rotor, the task of the designer is therefore to estimate the energy yield in the windy regime considered. The different wind turbines are characterized by the rated power value Pn, which constitutes the maximum electrical power produced by the electric generator. The corresponding rotor power value PRn is naturally higher due to the mechanical losses (slow and possible axle mechanical and mechanical seals) and electrical (generator, if any inverter) in the power transmission chain from the rotor to the grid electricity. Indicative value, for modern wind turbines, of global mechanical losses is around 4%; The output of a generator is about 0.96 to 0.97, and that of a frequency converter 0.97 to 0.98. Of course, for economic considerations, the nominal power of a wind turbine is far below the power value it could produce at the highest wind speeds. When the wind speed is between the nominal value v1n and the maximum speed at which the rotor is operated (deceleration or cut-out speed), it is necessary to check the power output of the rotor constantly at the PRn value (or at lower values). For wind speeds below the nominal value v1n, the rotor will operate under partial yield conditions. The nominal speed value v1n and therefore the choice of nominal power value meets the criteria of technical-economic optimization, and constitutes a fundamental design choice for a wind generator. All the wind generators connected to a mains power supply up to a decade ago are of the type with an electric generator directly connected to the grid, and therefore have to operate under all circumstances with rotor at constant rotational speed, apart from modest consequent variations The sliding of any conventional asynchronous generator; The speed of rotation is determined by the network frequency, the number of polar pairs of the electric generator, and of course the rotation speed multiplication ratio between the slow rotor axis and the fastener axis of the generator. This prevents the value of the peripheral speed ratio from being adjusted to the wind speed value; Only for a wind speed value the rotor can operate at the maximum value of the power coefficient. Determining the constant rotor speed that renders maximum energy yield naturally requires knowledge of the frequency distribution of wind speed. The rotor speed and the rated power of the generator then determine the nominal operating point in the characteristic curve of the rotor power coefficient; This point usually falls to the left of the maximum value point of the rotor power coefficient. For aerogenerators with the possibility of motion control of the blade pitch, in the full power range (to the left of the nominal operating point in the CPR - λ diagram) the power is controlled at the nominal value by variation of the bevel angle of the blades. In partial yield operation (to the right of the nominal operating point in the CPR - λ diagram), it can still be operated by varying the step of the blades in search of optimum operating conditions, but this requires a complex adaptive control system; It is generally preferred to operate at a suitable constant value of the step of the blades.

The operating curve in the CPR - λ diagram of a three - blade real - purpose wind turbine (WKA - 60) as described above is shown in *Figure 3*0 his is a German experimental wind turbine with a nominal electric power 1200 kW (rotoric 1342 kW), rotor diameter D = 60 m, wind speed cut-in-cut-out 6 - 24 m s-1, Wind speed v1n = 12 m s-1, fixed rotation speed Ng = 23 rpm

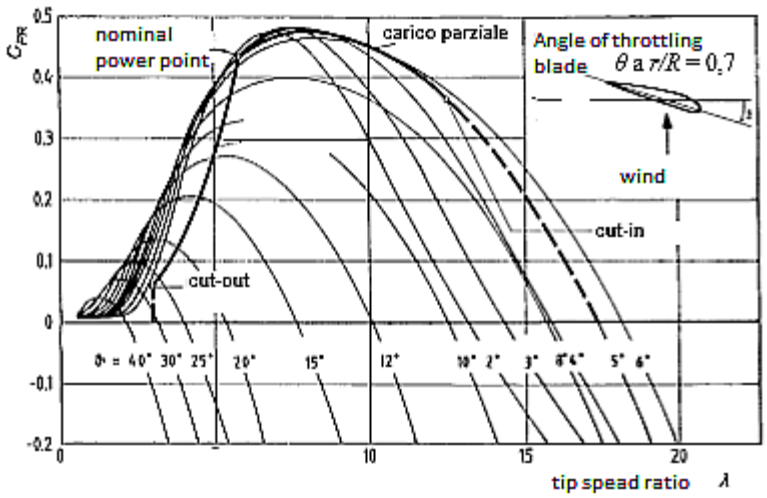


*figure30: dependence of Cpr frome Tip speed ration in a real macchine*

From the relationship of CPR dependence on λ, it is immediately possible to obtain rotor power as a function of wind speed; The diagram is shown in *Figure 31*.

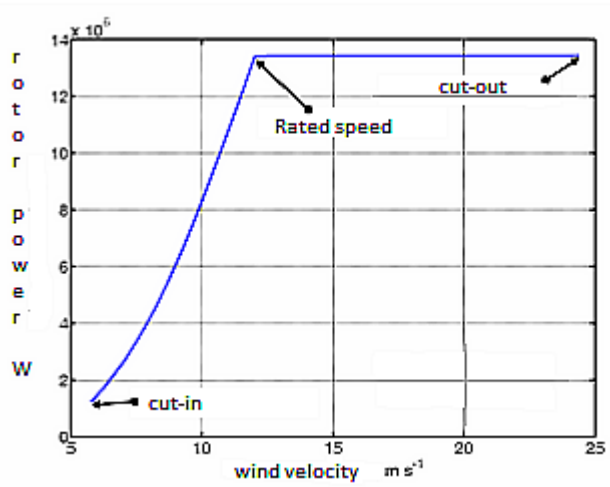


*figure31: variation of rotor power of wind turbine and wind velocity*

In order to derive the energy yield (producibility) of a wind turbine, the statistical distribution of the wind during the period considered has to be taken into account, for example through Weibull's statistical functions.
The procedure is simple: total energy production E in the time period Δτ (the usual reference is one year) is obtained by integrating instantaneous power P as follows(Eq.82):

$$E = \int_{\Delta\tau} P(\tau)d\tau \qquad (82)$$

That, it can write (Eq.83):

$$E = \Delta\tau \int_{v_{cut-in}}^{v_{cut-out}} P(\tau)D(v)dv \qquad (83)$$

The function integrated in (83) is called power density shows the distribution of wind power collected from the rotor as a function of wind speed. By referring to the power density of the rotor disk area unit, the specific power density is obtained. Also with reference to the already considered wind turbine WKA60, and considering an annual wind distribution that can be represented by Weibull's function with k = 2 factor factor and s = 7.9 m s-1 scale factor, *Figure 32* is represented The specific power density captured by the rotor; The same diagram also shows the specific power density available in the wind, and the maximum capture rate according to Betz.

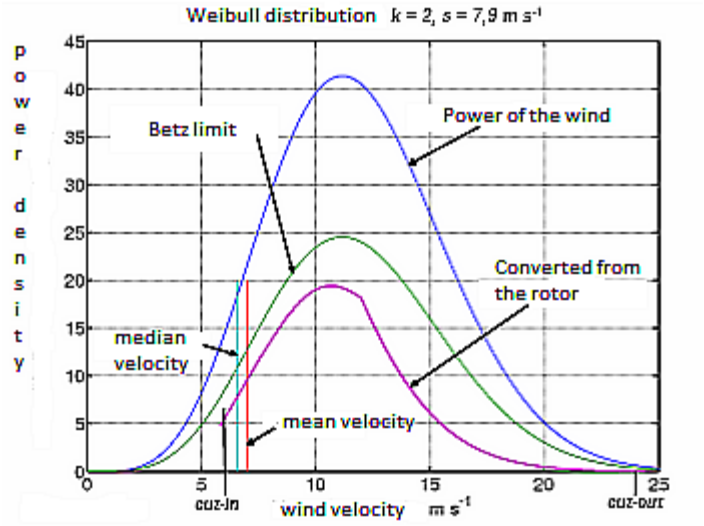


*Figure32: specific power density captured by the rotor*

Examining *figure 32* highlights some important facts:

- The loss of energy due to wind turbine arrest for wind speeds above the cut-out speed (24 m s-1) is absolutely negligible.
- The same can not be said of failure to recover wind power at wind speeds lower than the cut-in speed (6 m s-1); This is due to the high value of the cut-in speed of this aerogenerator (which is justified by its experimental character). Usually, the value of the peripheral cut-in velocity ratio is closest to the escape value (value at which the power coefficient on the right side of the CPR - λ curve is abolished, see *figure 31*); Usual speed cut-in speeds for wind turbines of this size are between 4 and 5 m s-1. In fact, if you could operate with 4.5 m s-1 cut-in speeds, following the fixed cutoff figure in *Figure 31* of the CPR (λ) curve, the annual energy captured at the rotor would go up to 3523 MWh / year, With an increase of more than 3%; The annual specific productivity would rise to 2626 h / year.
- The maximum energy collection is for wind speeds between 7 and 13 m s-1.

In recent times, wind generators with an electric generator (connected to the grid) have been developed asynchronous with rotor windings and sliding rings that allow connection of rotor windings to external power converter. Controlling the power of rotor windings allows the rotor slider, and hence its rotation speed, to vary within wide margins. The wind turbine can consequently be operated, in partial yield operation (speed of Wind below nominal speed) at variable speeds, proportional to wind speed. In this way the wind turbine can be operated in this wind speed regime, constantly at the maximum value of the CPR rotor power coefficient. Another advantage in using an asynchronous generator with rotor

winding is the ability to control reactive power absorption. The same advantages for the wind turbine (possibility of being operated at variable speed rotation and reactive power control) are achieved by the use of a high voltage synchronous electric generator with a high number of polar pairs (up to one hundred) and a converter. This latter electronic power transformer transforms the variable frequency current generated by the DC generator, and subsequently (inverters and electronic switches) in AC power that is suitable for powering the network. A major advantage of this solution is the elimination of the speed multiplier, with its direct and indirect costs (for the considerable mass).
The management of a wind turbine at variable speeds in the wind speed range between the cut-in and the nominal speeds allows to improve the annual energy yield. With reference to the same characteristics as the wind turbine in *Figures 31 to 33 Figure 34* shows the comparison of the power curves between fixed and variable rotational speed management; *Figure 35* shows the same comparison with regard to the power density, with reference to the same statistical wind distribution. Annual energy productivity, with variable speed rotation management, is 3486 MWh / year; Significant improvements would be achieved for lower cut-in speeds: with vcut-in = 4.5 m s-1, the annual productivity between variable and fixed rotation speeds would increase by almost 4%.

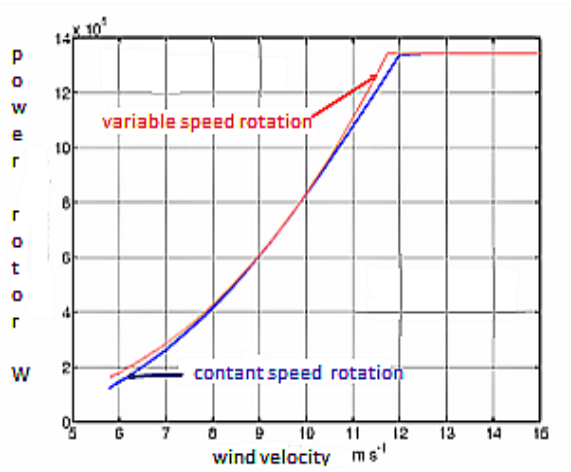

*figure34: variable speed rotation effect*

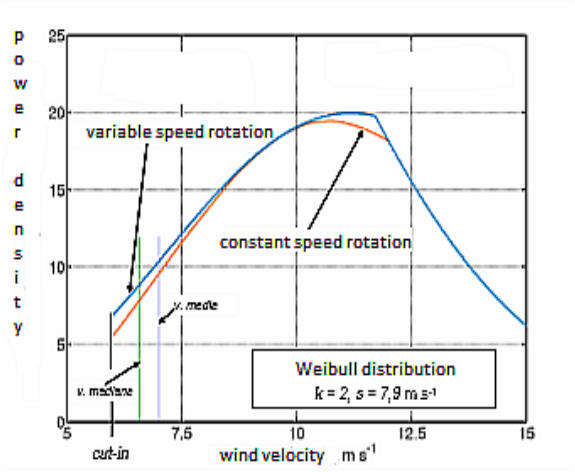

*figure35: variable speed rotation effect*

# 5 Es milà eolic park

The practical case of this thesis refers to an existing wind farm located on the island of Minorca in the municipality of Mahon (Latitud: 39° 55' 11.2" - Longitude: 4° 15' 4.9"). The wind farm is called “Es Milà” and it is the first and the only one built in the Balearic Islands. The wind farm is owned and operated by “Consorcio RSU Menorca”.

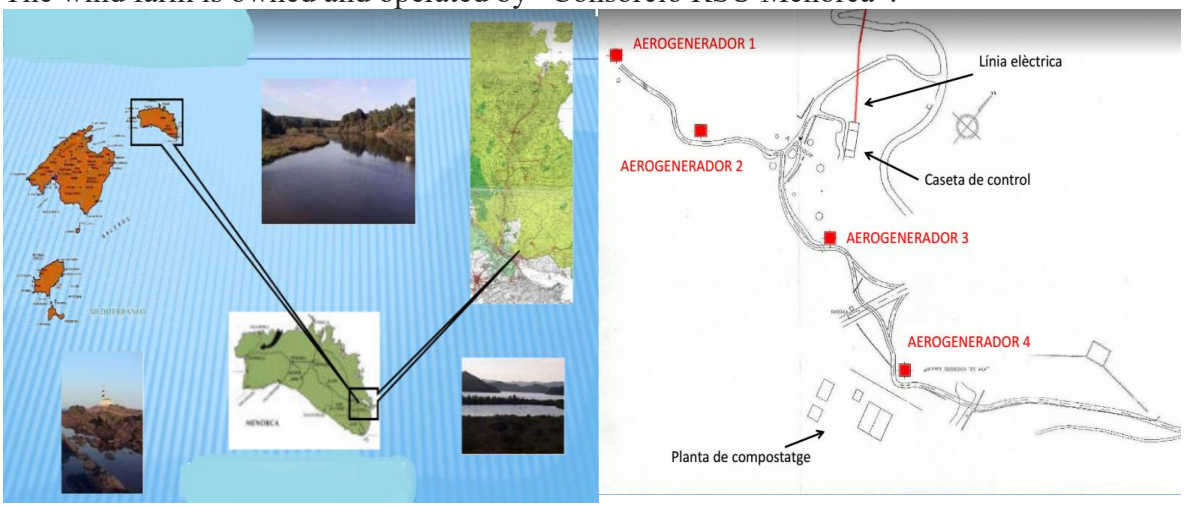


The park consists of four wind turbines, the technical data are:

| | |
|---|---|
| **Total installed power** | **3,2 [MW]** |
| **Nominal power (one turbine)** | **800 [kW]** |
| **Expected production** | **7040 [MWh/year]** |
| **Tower height** | **50 [m]** |
| **Diameter of blades** | **59 [m]** |
| **total height** | **79,50 [m]** |
| **total weight** | **87000 [kg]** |
| **Cut-in velocity** | **3,1 [m/s]** |
| **Maximun performance velocity** | **11 [m/s]** |
| **Cut-out velocity** | **25 [m/s]** |
| **Production of CO2 avoided** | **6600 [t/year]** |
| **Start production** | **February 2004** |
| **Useful life** | **20 year** |

# 6 Experimental data analysis

## 6.1 Wind Rose

The study of the wind rose is very important to know the wind direction on a given site.
It is especially important in a wind farm to evaluate the ideal locations where the turbines should be placed, so that they interfere with each other as little as possible. The data of the various measuring stations divide the wind directions into sixteen angular areas.
We will refer to three types of roses of the winds:
The first will tell us the frequency for each possible wind direction (blue), for wind applications is the least significant, surely it is more interesting to filter the wind direction frequency only when the wind turbine can actually operate or delete all the direction data for the wind Such as wind speed is inferior to the cut speed in or greater than the cut-out speed (red).
The second type is weighed on the wind speed value for each direction considered, which tells us how much it affects each direction at the average wind speed.
The third type of wind rose, weighed on the wind speed cube, tells us how much the wind power affects each direction. This is the most important of all for wind power applications. Is the one on which the choice of the relative positions of wind turbines is based on optimizing energy production. If wind energy does not have preferential directions but is evenly distributed in all directions, it may indicate that the site in question is not suitable for the construction of a wind farm. In the directions for which wind power is the most, the turbines should not interfere with each other or do so as little as possible. It is a good idea to place the turbines in the normal direction to the maximum wind power direction. The three wind roots described above are calculated annually for each measuring station.
It is important to remember that there is a basic hypothesis that the wind direction measured by the stations coincides with the direction of the wind where the turbine operates. It is a hypostasis that is often verified but that it is not assumed that it is certain. There are no valid and generalized mathematical models to say how the wind direction can change with height.

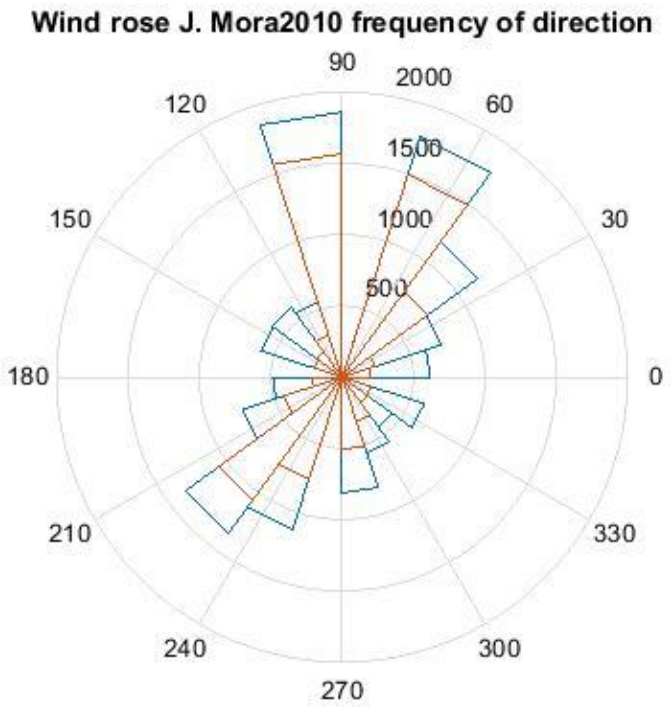
Wind rose J. Mora2010 frequency of direction
90
2000
60
120
1500
150
1000
30
500
180
0
210
330
240
300
270

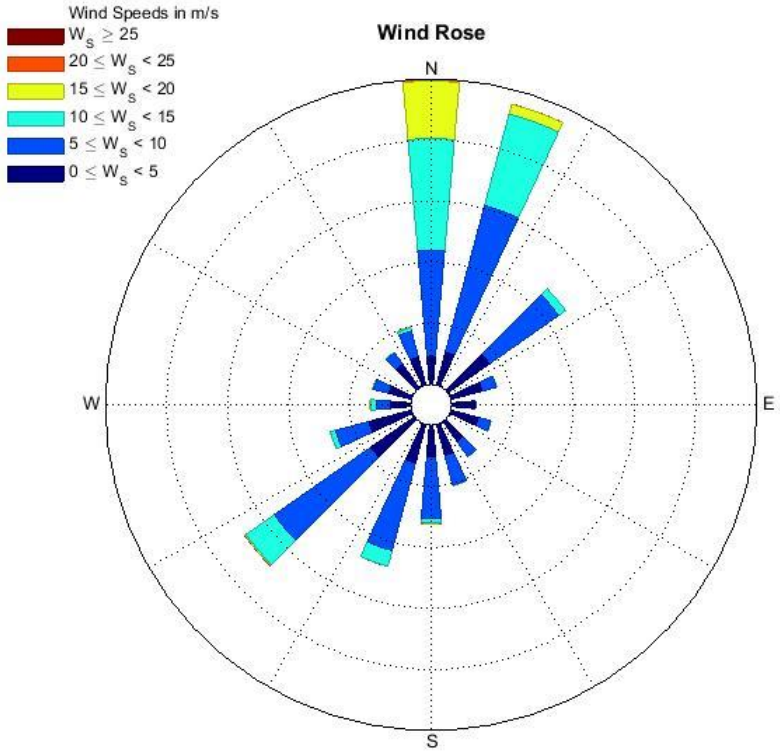
Wind Speeds in m/s
W_S ≥ 25
20 ≤ W_S < 25
15 ≤ W_S < 20
10 ≤ W_S < 15
5 ≤ W_S < 10
0 ≤ W_S < 5
Wind Rose
N
W
E
S

**J. Mora 2010**

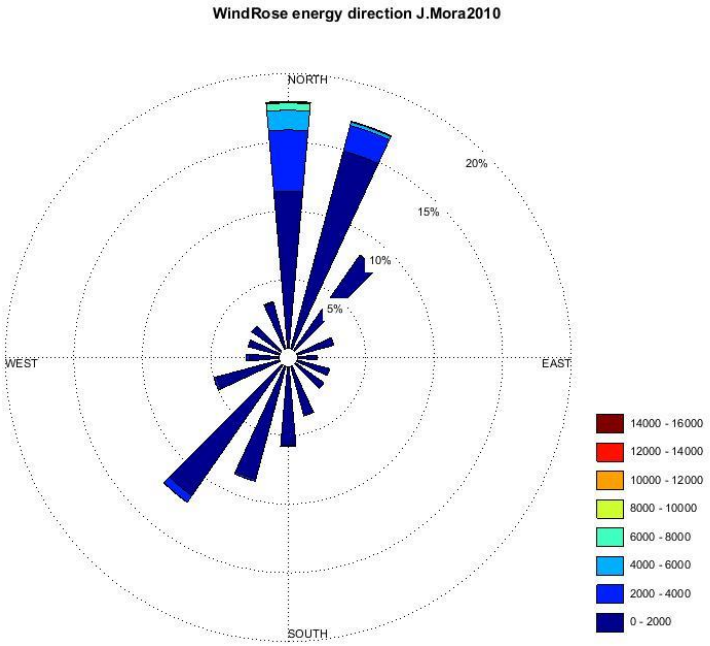
WindRose energy direction J.Mora2010
NORTH
20%
15%
10%
5%
WEST
EAST
SOUTH
14000 - 16000
12000 - 14000
10000 - 12000
8000 - 10000
6000 - 8000
4000 - 6000
2000 - 4000
0 - 2000

## J. Mora 2011

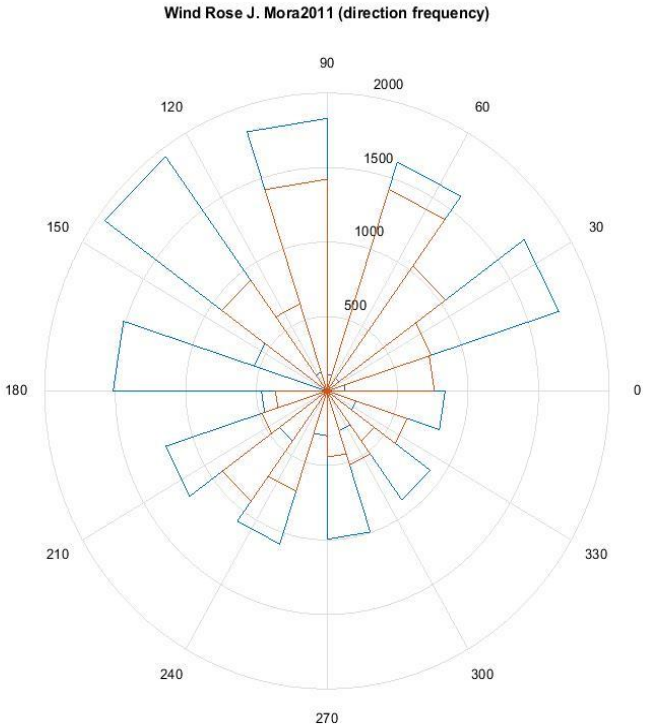
Wind Rose J. Mora2011 (direction frequency)
90
2000
60
120
1500
30
150
1000
500
180
0
210
330
240
300
270

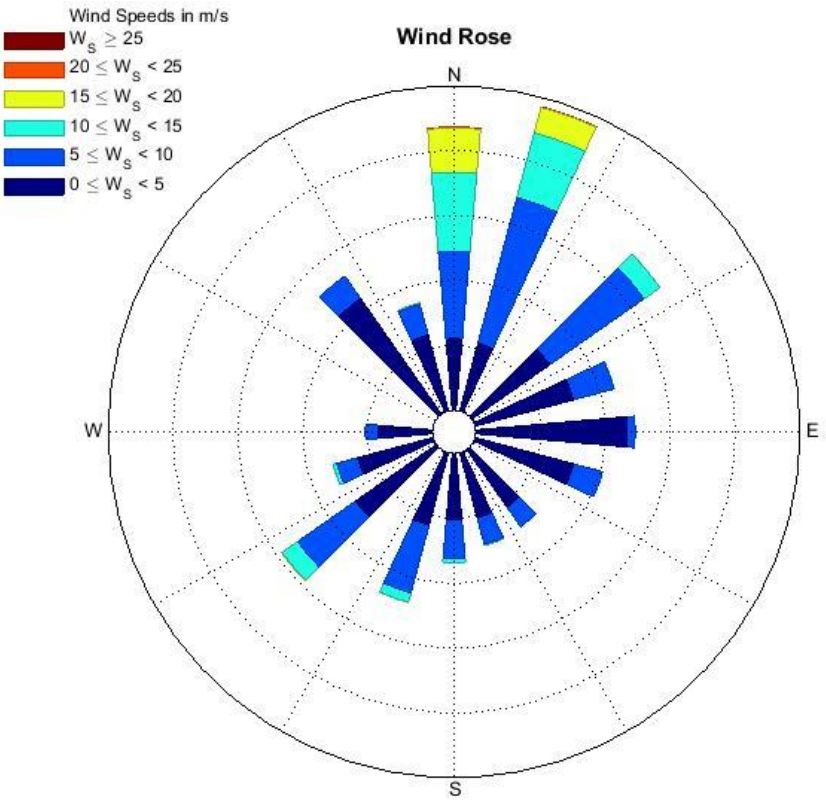
Wind Speeds in m/s
$W_S \geq 25$
$20 \leq W_S < 25$
$15 \leq W_S < 20$
$10 \leq W_S < 15$
$5 \leq W_S < 10$
$0 \leq W_S < 5$
Wind Rose
N
W
E
S

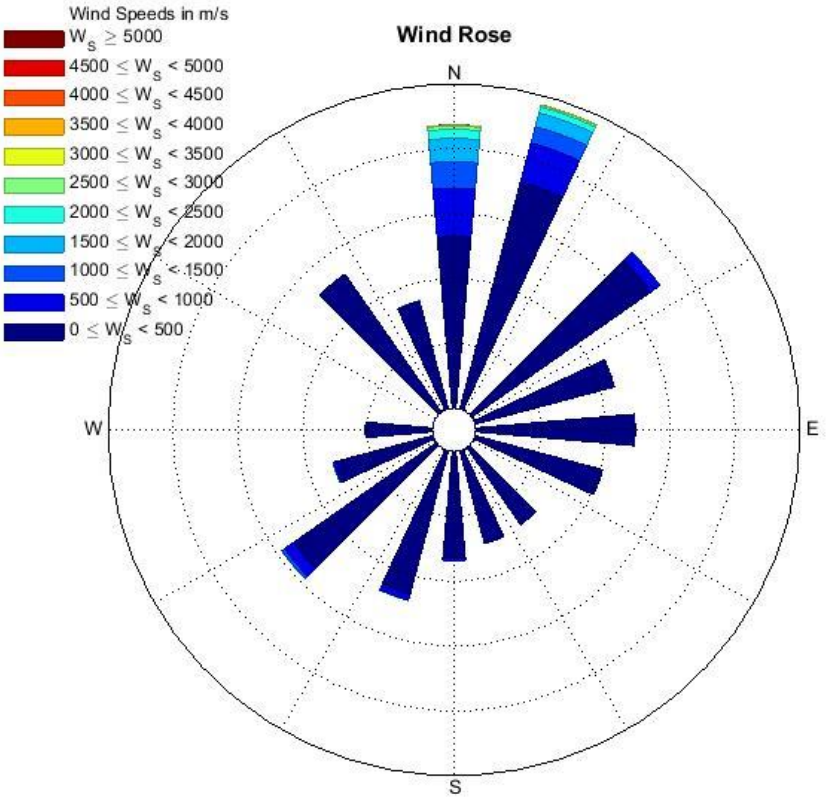
Wind Speeds in m/s
$W_S \geq 5000$
$4500 \leq W_S < 5000$
$4000 \leq W_S < 4500$
$3500 \leq W_S < 4000$
$3000 \leq W_S < 3500$
$2500 \leq W_S < 3000$
$2000 \leq W_S < 2500$
$1500 \leq W_S < 2000$
$1000 \leq W_S < 1500$
$500 \leq W_S < 1000$
$0 \leq W_S < 500$
Wind Rose
N
W
E
S

**J. Mora2012**

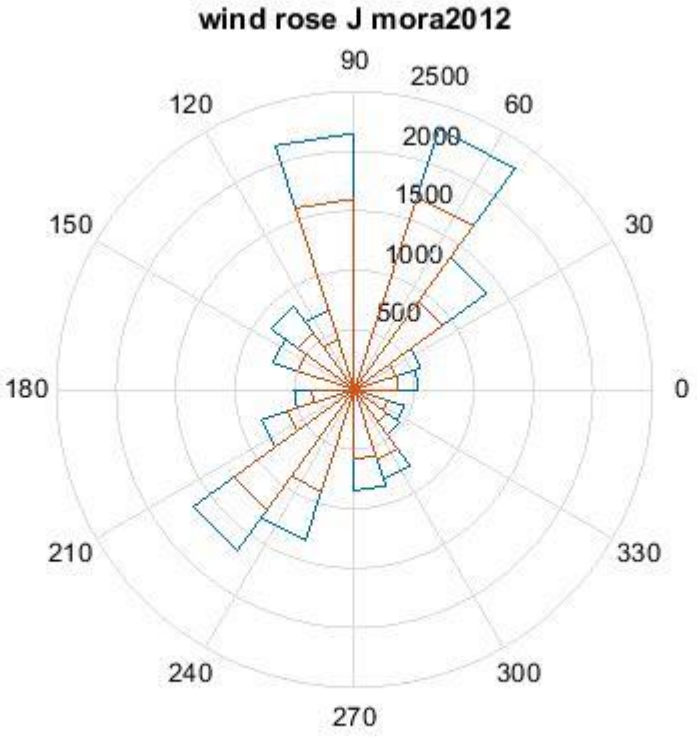
wind rose J mora2012
90
2500
60
120
2000
1500
150
30
1000
500
180
0
210
330
240
300
270

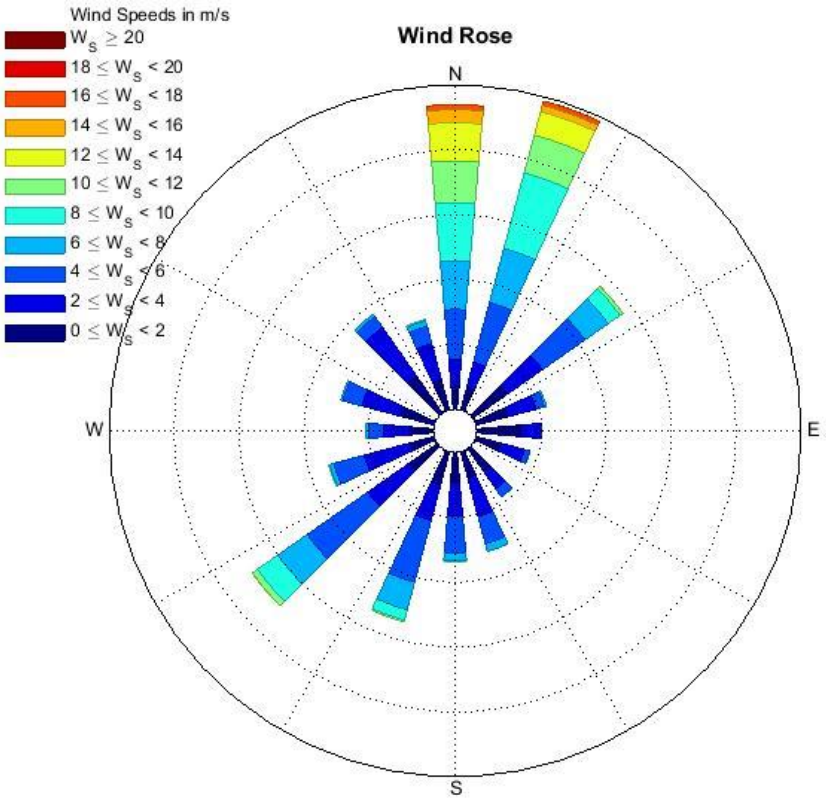
Wind Speeds in m/s
W_S ≥ 20
18 ≤ W_S < 20
16 ≤ W_S < 18
14 ≤ W_S < 16
12 ≤ W_S < 14
10 ≤ W_S < 12
8 ≤ W_S < 10
6 ≤ W_S < 8
4 ≤ W_S < 6
2 ≤ W_S < 4
0 ≤ W_S < 2
Wind Rose
N
W
E
S

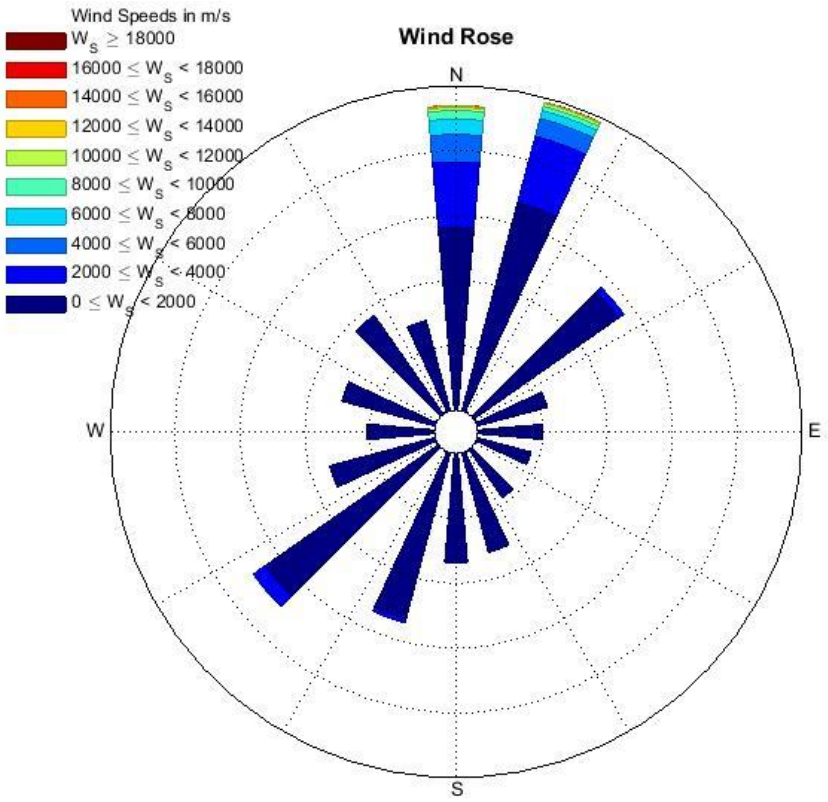
Wind Speeds in m/s
$W_S \geq 18000$
$16000 \leq W_S < 18000$
$14000 \leq W_S < 16000$
$12000 \leq W_S < 14000$
$10000 \leq W_S < 12000$
$8000 \leq W_S < 10000$
$6000 \leq W_S < 8000$
$4000 \leq W_S < 6000$
$2000 \leq W_S < 4000$
$0 \leq W_S < 2000$
Wind Rose
N
W
E
S

**J. Mora 2013**

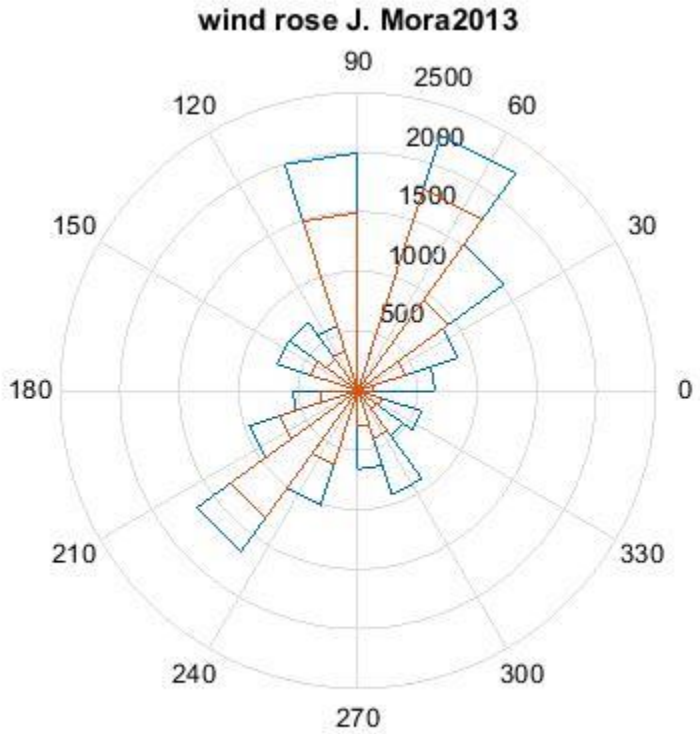
wind rose J. Mora2013
90
2500
60
120
2000
1500
150
30
1000
500
180
0
210
330
240
300
270

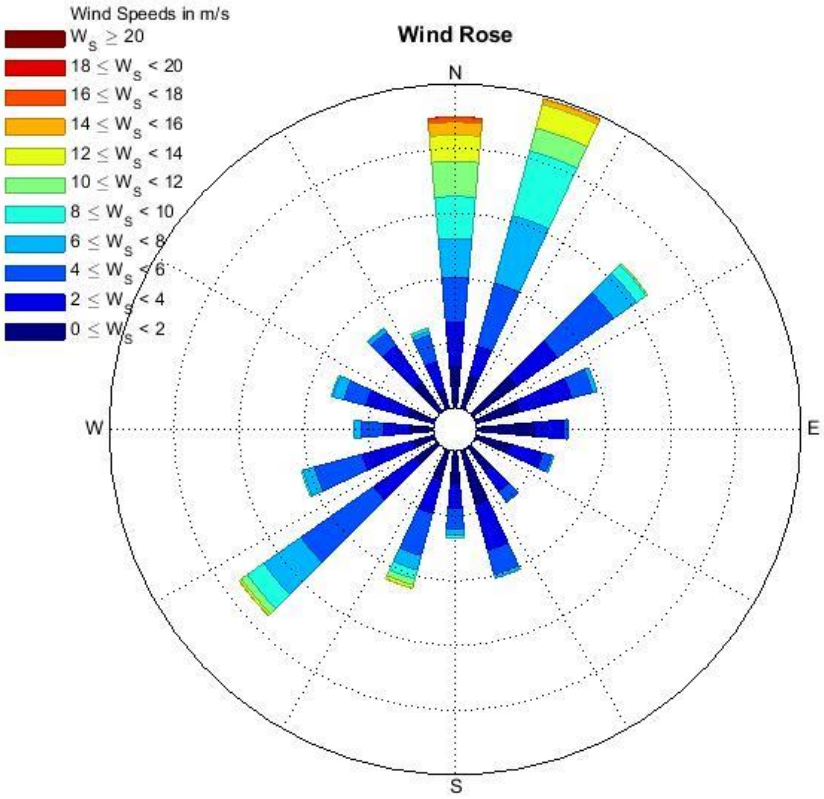
Wind Speeds in m/s
$W_S \geq 20$
$18 \leq W_S < 20$
$16 \leq W_S < 18$
$14 \leq W_S < 16$
$12 \leq W_S < 14$
$10 \leq W_S < 12$
$8 \leq W_S < 10$
$6 \leq W_S < 8$
$4 \leq W_S < 6$
$2 \leq W_S < 4$
$0 \leq W_S < 2$
Wind Rose
N
W
E
S

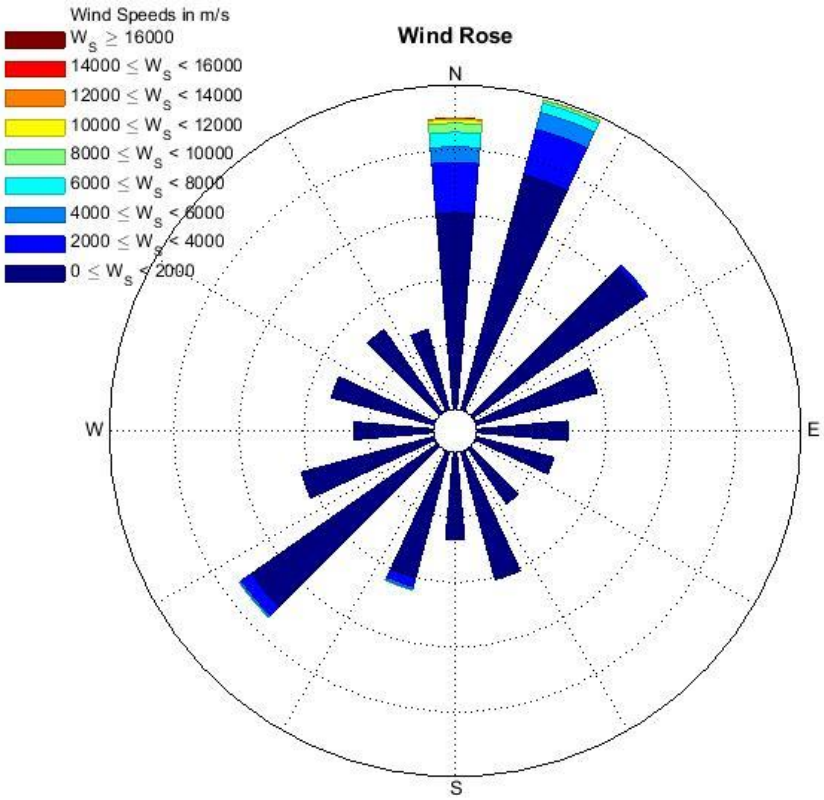
Wind Speeds in m/s
$W_S \geq 16000$
$14000 \leq W_S < 16000$
$12000 \leq W_S < 14000$
$10000 \leq W_S < 12000$
$8000 \leq W_S < 10000$
$6000 \leq W_S < 8000$
$4000 \leq W_S < 6000$
$2000 \leq W_S < 4000$
$0 \leq W_S < 2000$
Wind Rose
N
W
E
S

**J.Mora 2014**

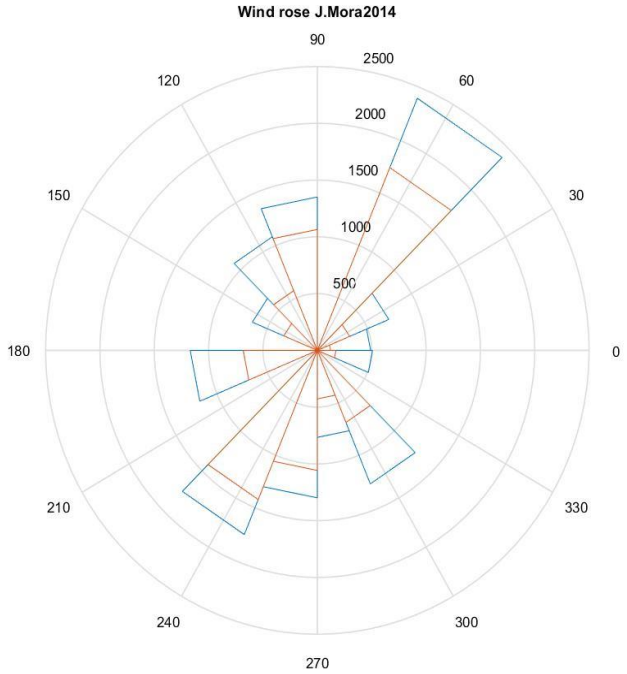
Wind rose J.Mora2014
90
2500
60
120
2000
1500
150
30
1000
500
180
0
210
330
240
300
270

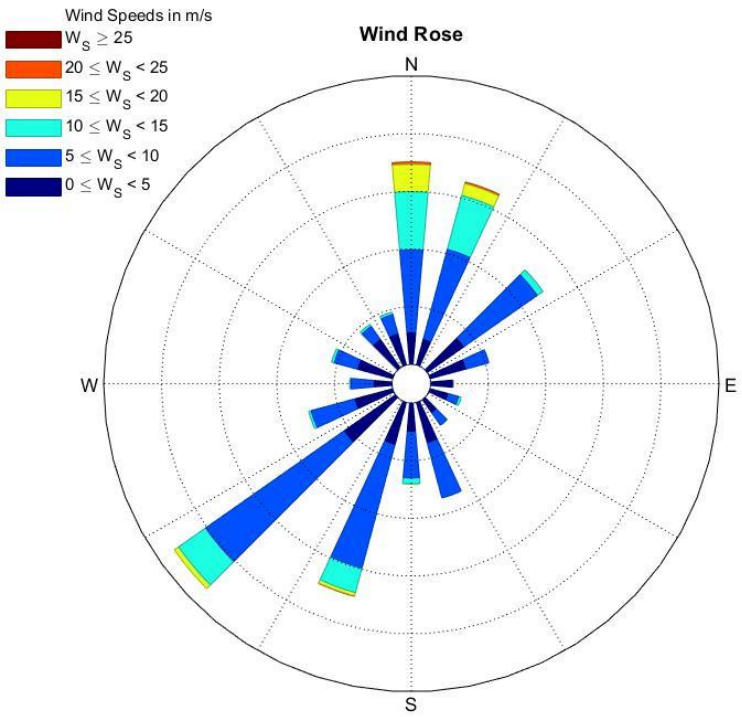
Wind Speeds in m/s
W_S ≥ 25
20 ≤ W_S < 25
15 ≤ W_S < 20
10 ≤ W_S < 15
5 ≤ W_S < 10
0 ≤ W_S < 5
Wind Rose
N
W
E
S

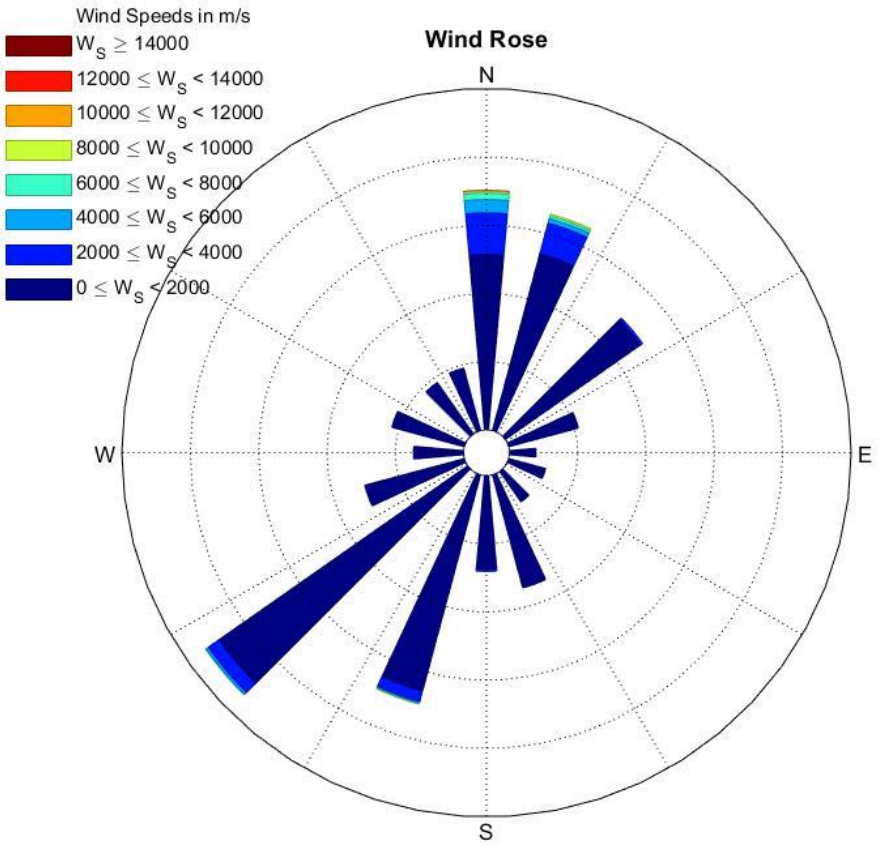


**Comments**

It is noted that the wind has a similar behavior in terms of direction on an annual basis. The wind's maximum energy directions are N-NE and SO, the fact that they are opposed to each other is probably due to the effect of the sea breeze. The turbines were placed in the optimum direction to minimize the interference between them along the maximum energy directions. In terms of frequency of direction as is well-evident in j. Mora 2011 wind graph. It must be, although there is a high probability that the wind comes from directions like NW, it often does not have significant speeds to operate the turbines, because they are lower than the cut-in ones.

## 6.2 Weibull analisys

To study the wind speed on a statistical basis, we will use the Weibull distribution (24), which is the most widely used wind study. It works well as the number of measurements made is high, as at least one month. Calculations are carried out on an annual basis.
The weibull distribution is based on two parameters, the form factor (k) and the scale factor (c), which can be calculated empirically by formulas (37) and (39) by knowing the average velocity and wind variance. The results are generally acceptable approximations. The most rigorous method for calculating weibull parameters is to solve equation (29) using the gamma function (28). The problem is that the form factor is implicitly contained in the gamma function and this makes it necessary to solve it with a numerical method. Fortunately in many computing software, as in MATLAB already there is the function to calculate numerically the weibull parameters. Through the weibull distribution it is possible to estimate the maximum wind energy speed to be used as design speeds for turbine design with the (36). Is also used to calculate wind energy (83) to express the probability for each velocity described by the distribution. The weibull distribution used uses the values of all the wind speeds > 0[m/s], extracted from the data of the various stations through the formula (9)

**Result**
**J. Mora2009**

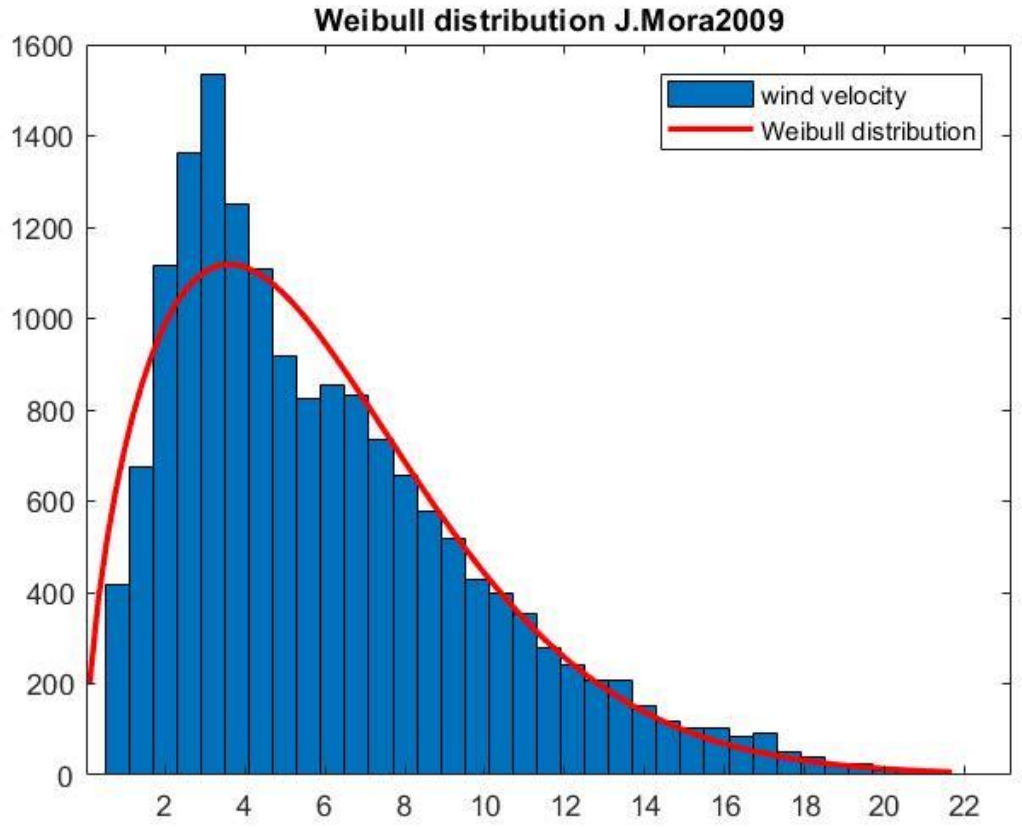


Weibull distribution parameters:

c= 6.65604
k= 1.59857
$v_e$= 11.0576 [m/s]

**J. Mora2010**

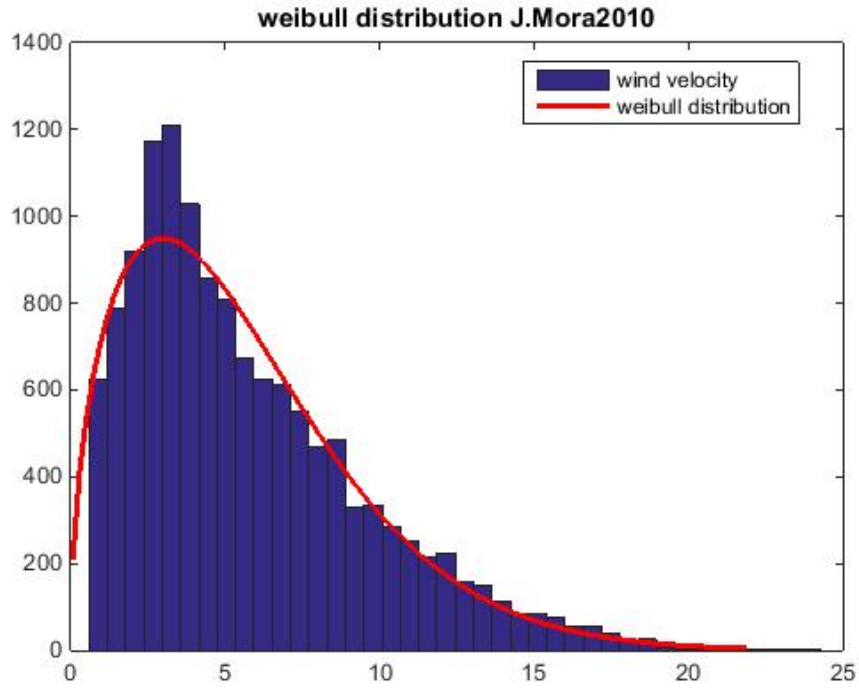


c=6,21111
k=1,4997
$v_e$ =11,1987[m/s]

**J. Mora 2011**

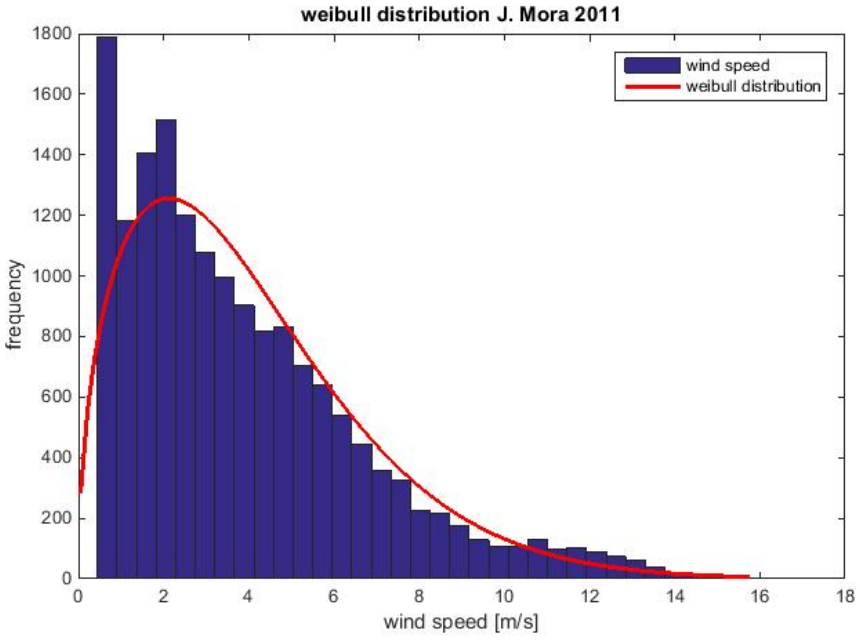

c= 6,04729
k= 1,49321
$v_e$ = 10,6845 [m/s]

**J. Mora2012**

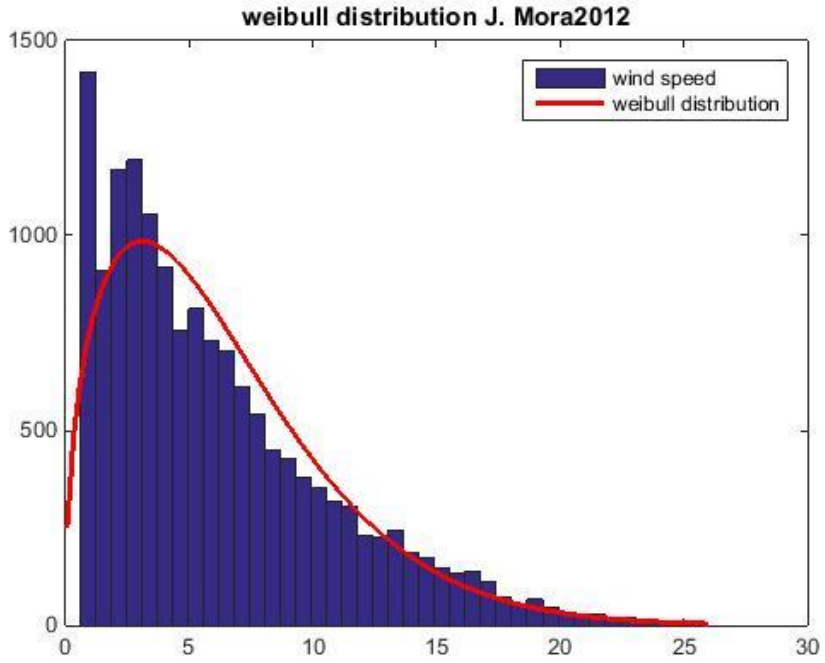


c= 7,02618
k= 1,44432
$v_e$ = 12,8247[m/s]

**J. Mora2013**

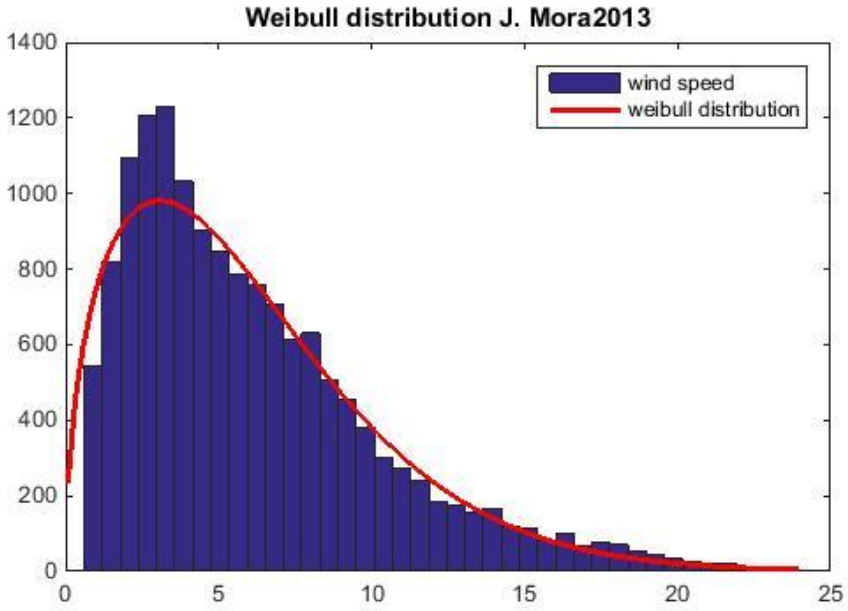


c= 6,65496
k= 1,47274

$v_e$ = 11.9153 [m/s]

**J.Mora2014**

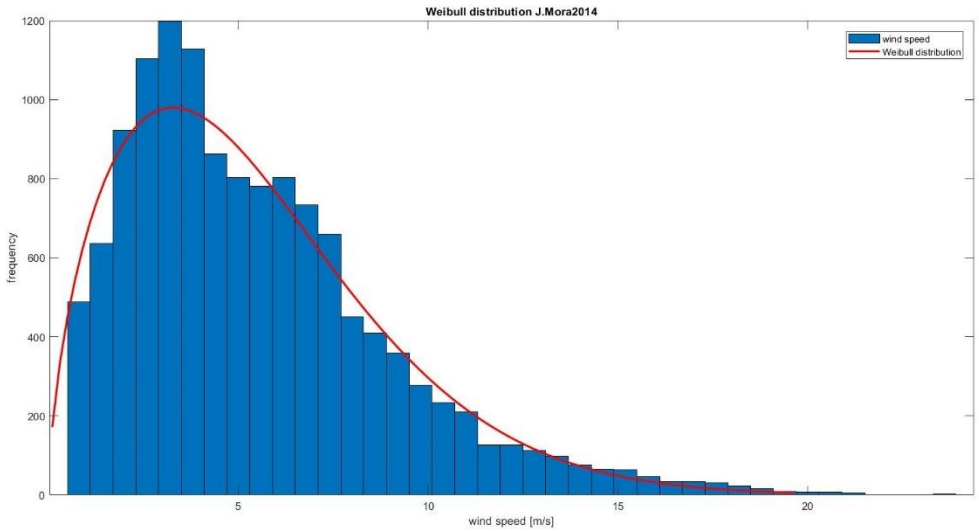


c =6,03951
k= 1,60267
$v_e$ = 10.0115 [m/s]

**Comments**
As we see from charts the weibull distribution describes well the wind speed on an annual basis. The wind speed calculated with the weibull distribution is around 11 [m / s], which is the one actually used for turbine design.

## 6.3 Calculation power and energy of wind

To calculate the wind power we refer to formula (33):

$$P_w = \frac{1}{2}\rho A u^3 \quad [W]$$

Where $\rho$ is the air density, $A$ is the area swept by the blades (sum of the area swept by the 4 turbines) and $u^3$is the cube of the speed of the wind considered constant in direction and intensity. The physical magnitudes (speed and density) that depend on the wind power are those where the turbines operate and are different from those measured by the various stations. We must therefore estimate them from the measured magnitudes and by making simplistic hypotheses to use the various mathematical models to calculate them.
Every power associated to each respective speed measure will be calculated, in order to calculate the wind energy, the power is multiplied for each time interval, considering therefore the wind speed and the respective power constant for each time interval. To calculate successively the theoretical energy provided by the model, it will suffice to multiply the calculated energy for each time interval for the corresponding value of the power coefficient

### 6.3.1 Air density calculation

For the calculation of air density, the ideal gas model has been hypothesed and the law of perfect gas status (4) will be considered valid. Having the temperature and pressure measurements of the air from the various stations the formula (5) will be used for calculating a density vector which will then be corrected by formula (6) to account for the height of the tower where the wind turbines operate. The influence of air humidity, which can be expressed by formula (7), will be neglected. The reason for this choice is that the variation in air density from its humidity is not as marked as dependence on temperature and pressure on it. Furthermore, there may also be significant variations in the humidity content of the air where the turbines operate compared to where it is measured, risking to deviate from the most accurate density estimate. Summing up the calculation hypothesis is to consider air as dry and ideal gas, these assumptions will probably lead to an overestimation of density. The various density vectors are calculated for each year and for each station, then the average value for each station and the average of the mean values will be calculated to arrive at a more verifiable estimate of the average annual density of the air. Since the temperature and pressure data for the year 2009 are not available, the average density for that year will be calculated as the average of the density values calculated for the other years.

## Result

### J. Mora station 2010

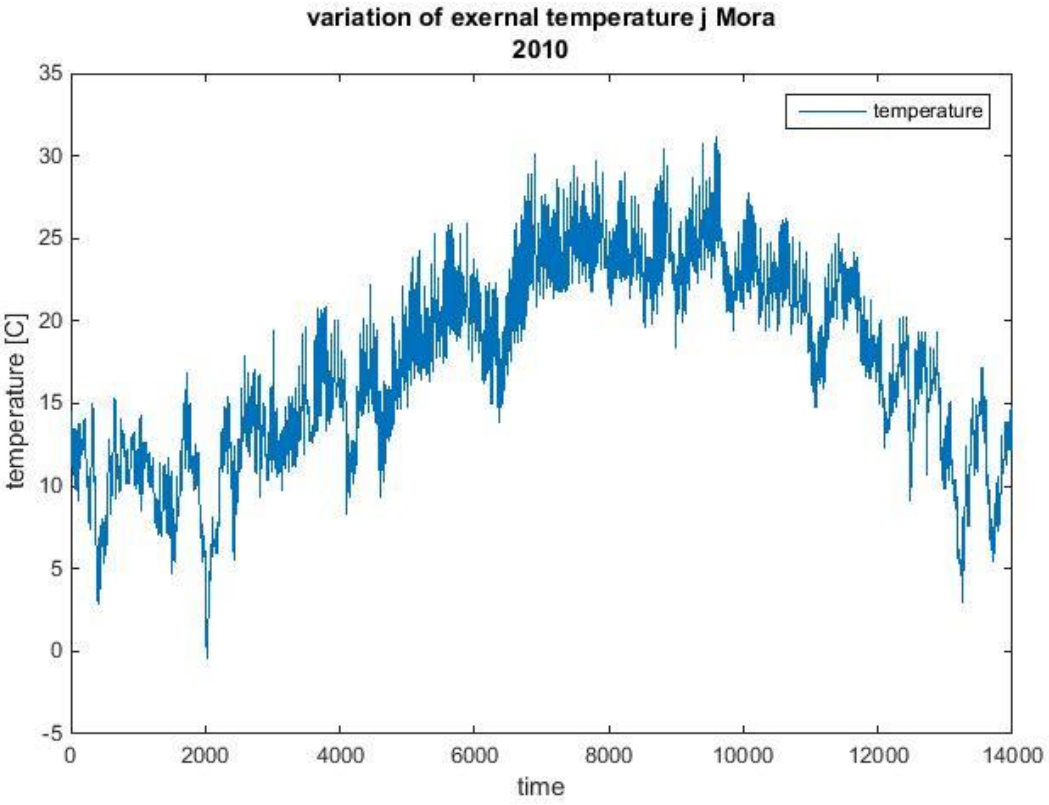

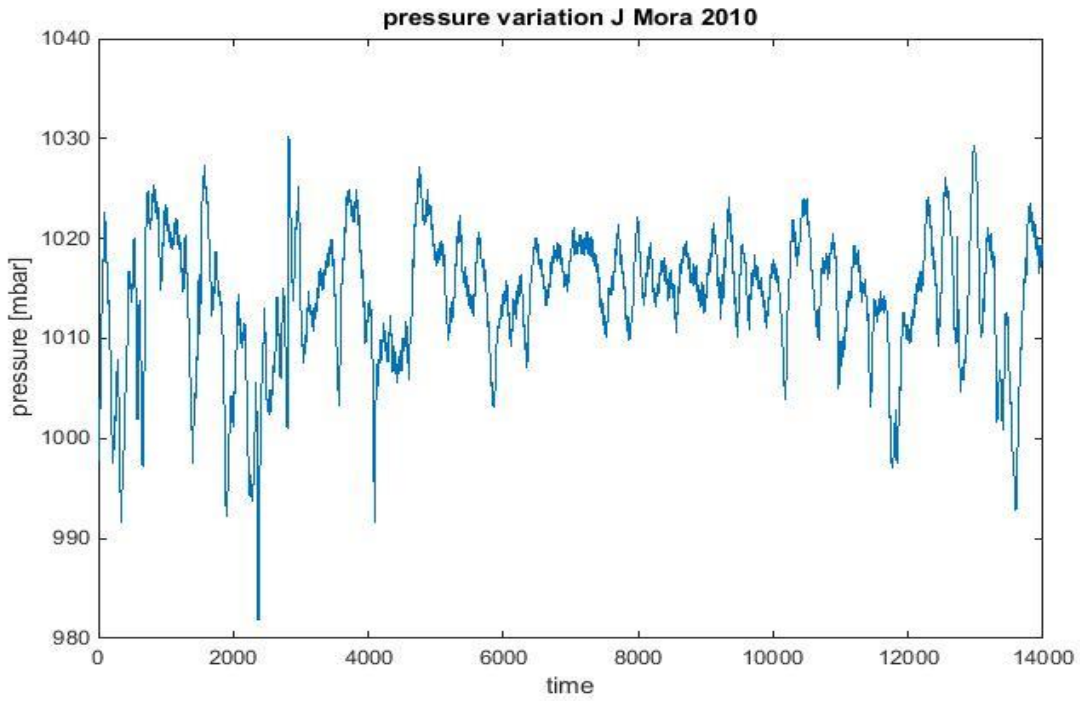


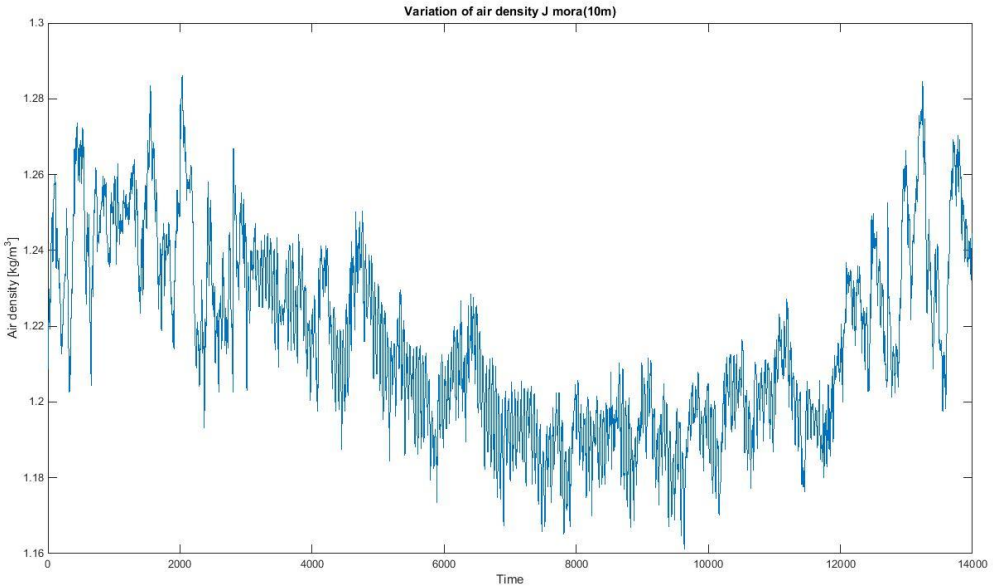


| | |
|---|---|
| Maximum density | 1.2799 [kg/m^3] |
| Minimum density | 1.1554 [kg/m^3] |
| **Mean density** | **1.2101[kg/m^3]** |

**J. Mora 2011**

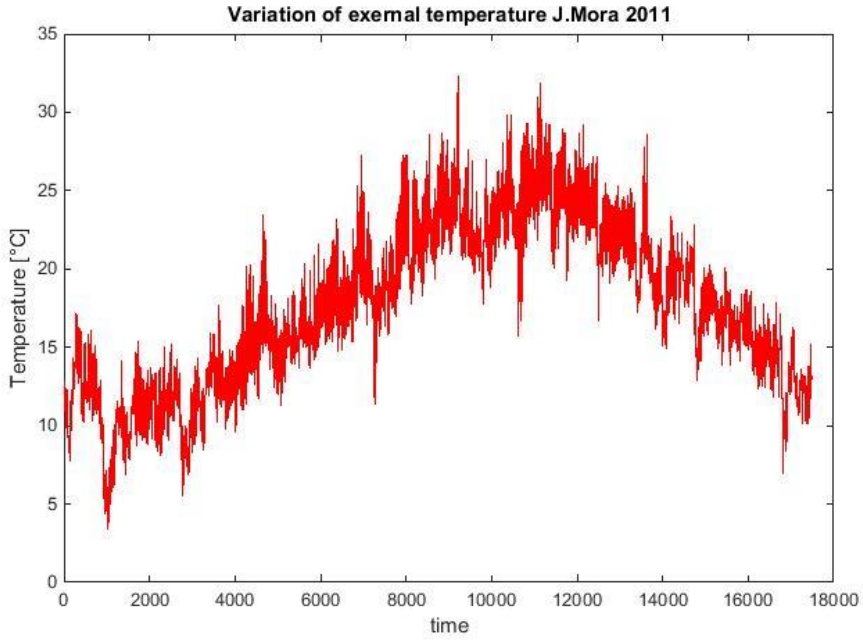
Variation of exernal temperature J.Mora 2011
Temperature [°C]
time
0
5
10
15
20
25
30
35
0
2000
4000
6000
8000
10000
12000
14000
16000
18000

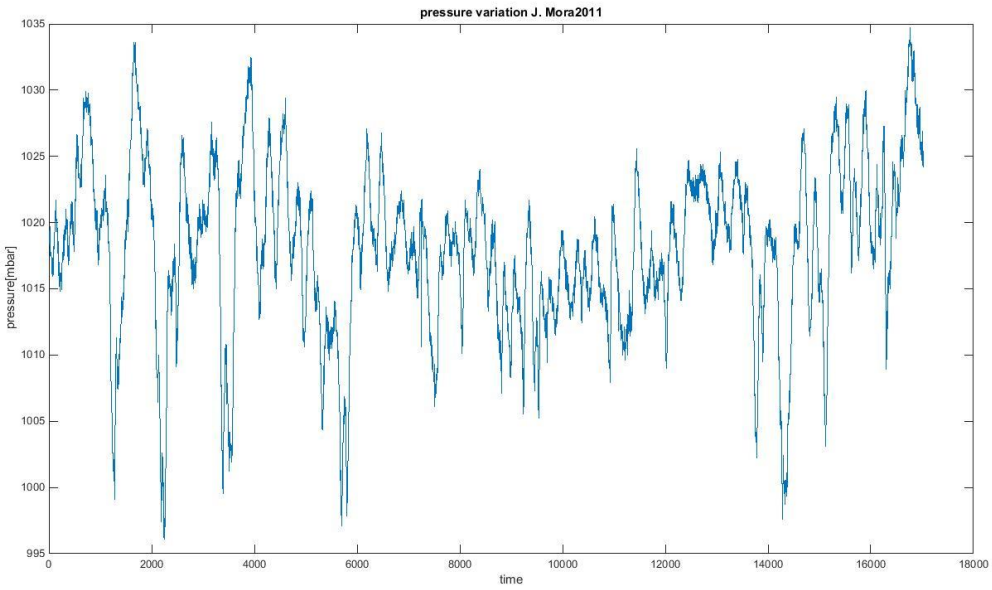
pressure variation J. Mora2011
pressure[mbar]
time
995
1000
1005
1010
1015
1020
1025
1030
1035
0
2000
4000
6000
8000
10000
12000
14000
16000
18000

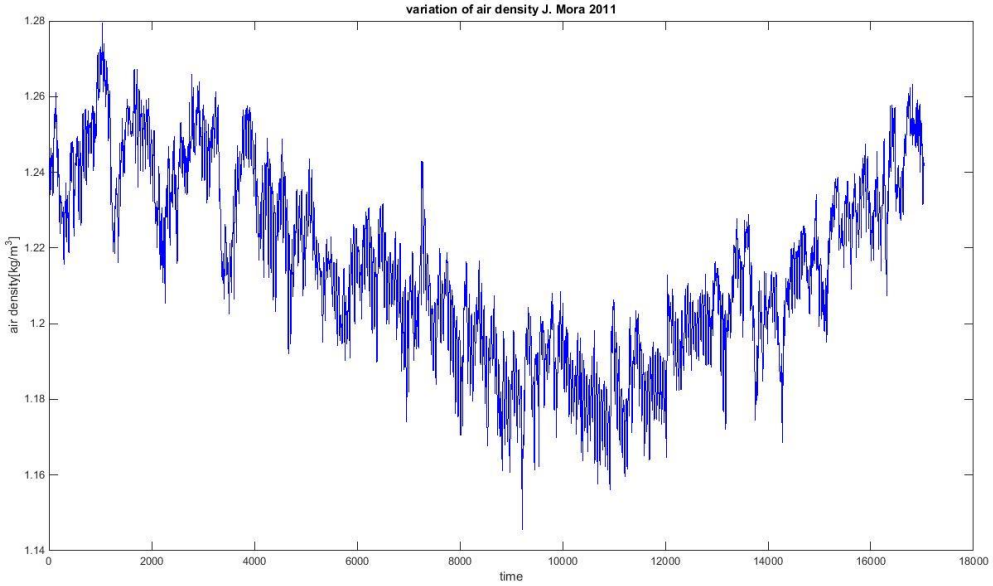


| | |
|---|---|
| Maximum density | 1,2795 [kg/m^3] |
| Minimum density | 1,1456 [kg/m^3] |
| **Mean density** | **1,2150 [kg/m^3]** |

**J. mora 2012**

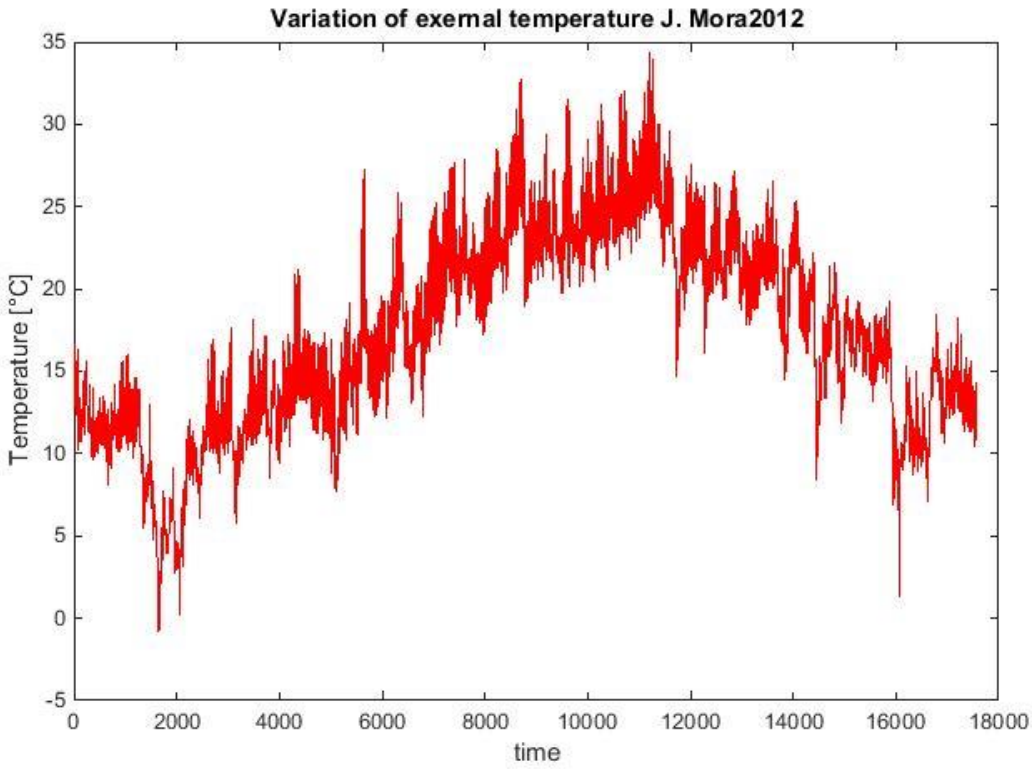
Variation of exernal temperature J. Mora2012
Temperature [°C]
time
35
30
25
20
15
10
5
0
-5
0
2000
4000
6000
8000
10000
12000
14000
16000
18000

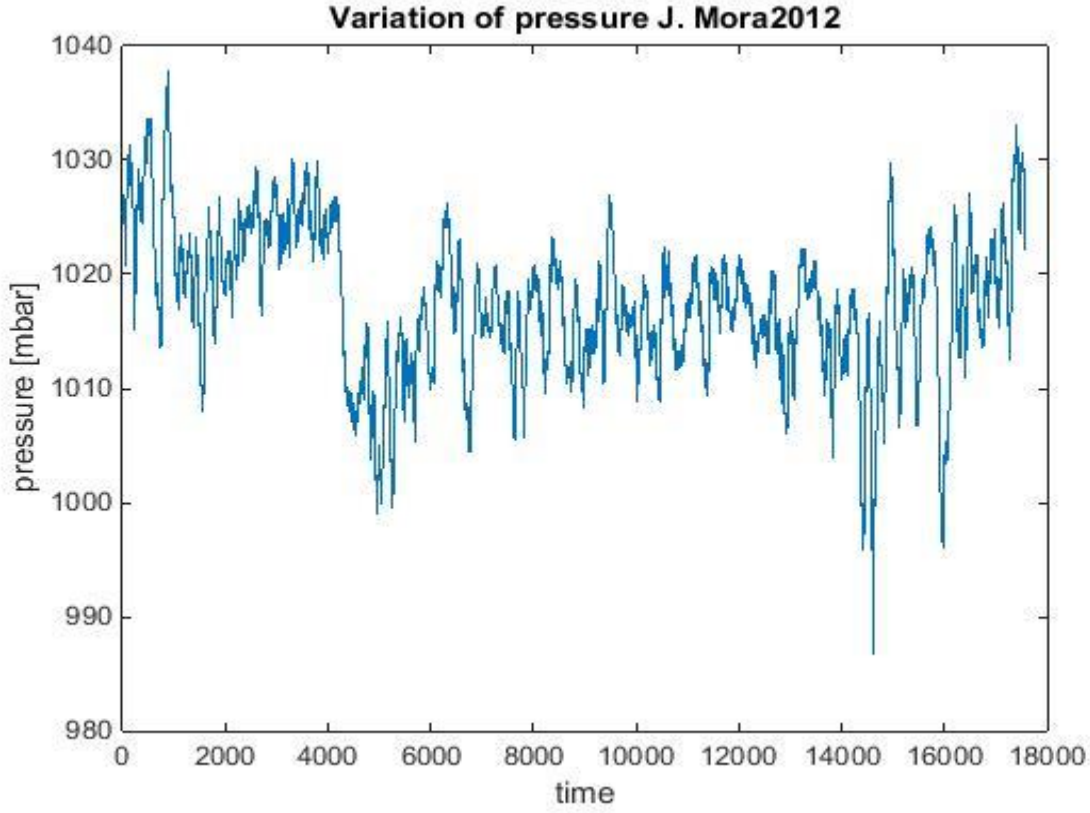
Variation of pressure J. Mora2012
pressure [mbar]
time
1040
1030
1020
1010
1000
990
980
0
2000
4000
6000
8000
10000
12000
14000
16000
18000

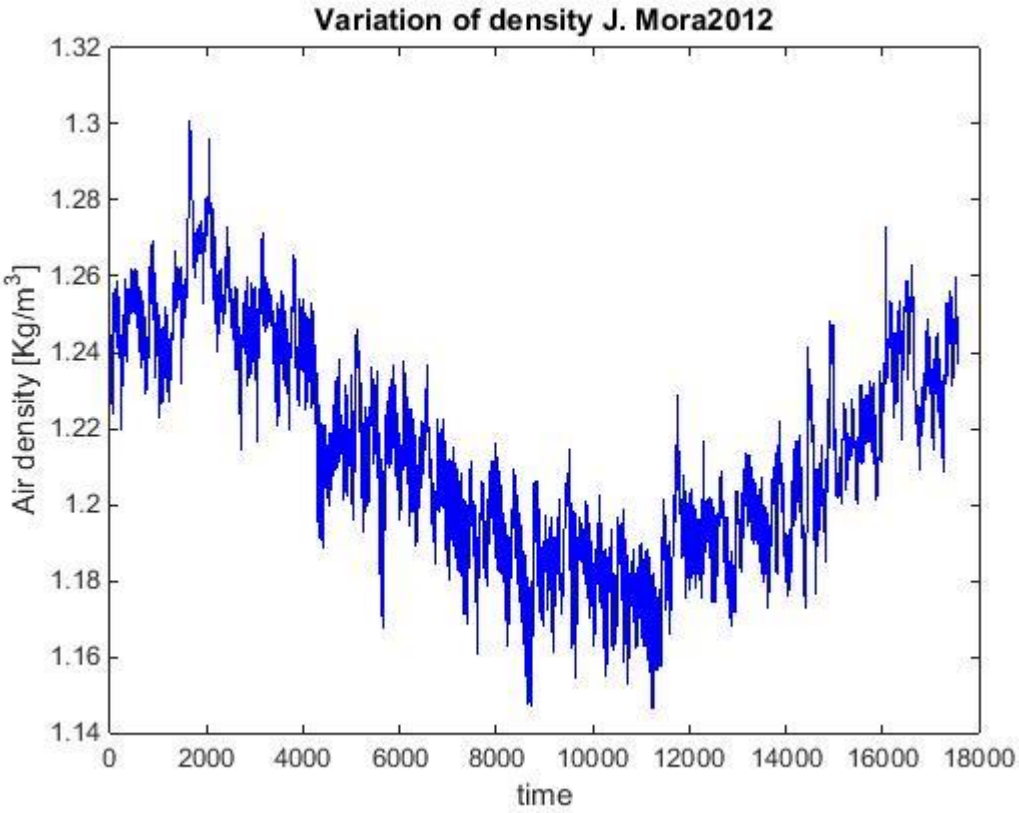


| | |
|---|---|
| Maximum density | 1,3011 [kg/m^3] |
| Minimum density | 1,1467 [kg/m^3] |
| **Mean density** | **1,2239 [kg/m^3]** |

**J. mora 2013**

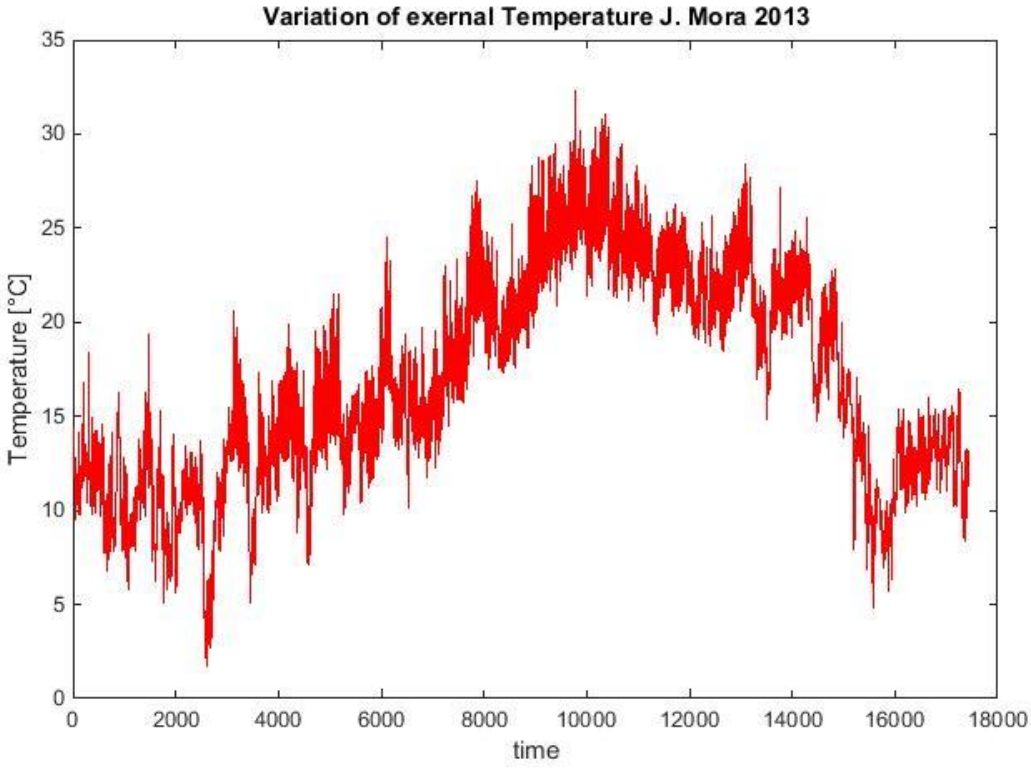
Variation of exernal Temperature J. Mora 2013
Temperature [°C]
time
0
5
10
15
20
25
30
35
0
2000
4000
6000
8000
10000
12000
14000
16000
18000

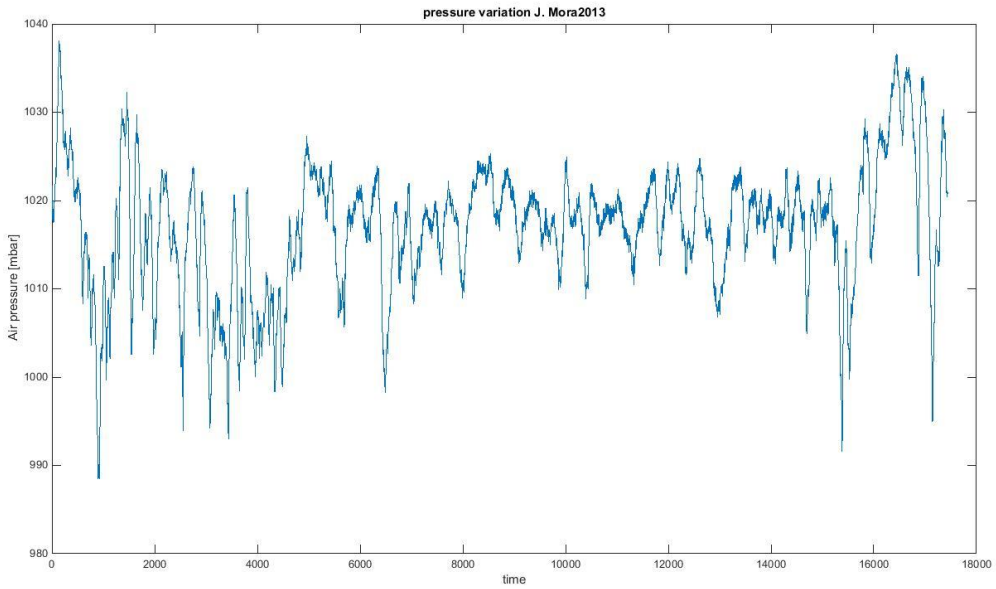
pressure variation J. Mora2013
Air pressure [mbar]
time
980
990
1000
1010
1020
1030
1040
0
2000
4000
6000
8000
10000
12000
14000
16000
18000

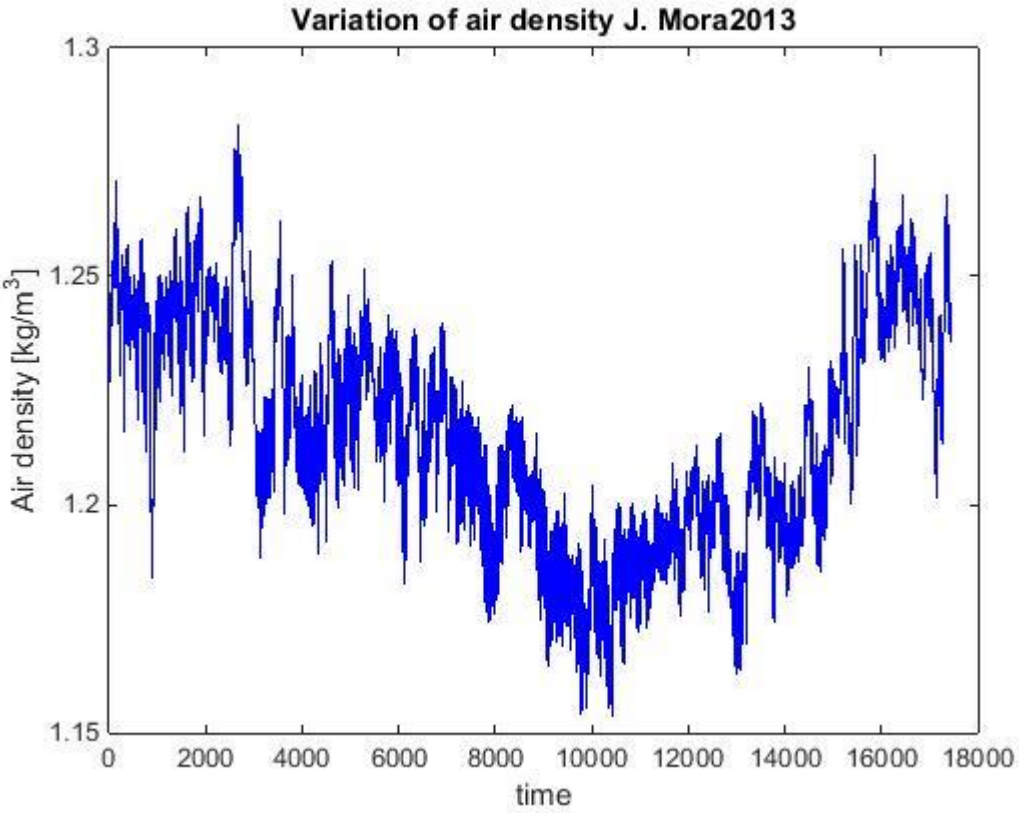


| | |
|---|---|
| Maximum density | 1,2831 [kg/m^3] |
| Minimum density | 1.1537 [kg/m^3] |
| **Mean density** | **1.2159 [kg/m^3]** |

**J.Mora2014**

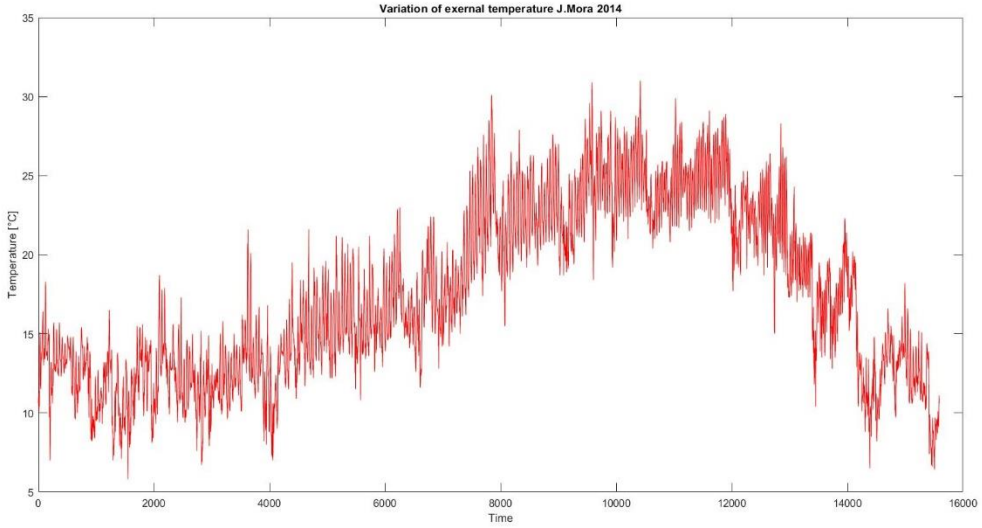

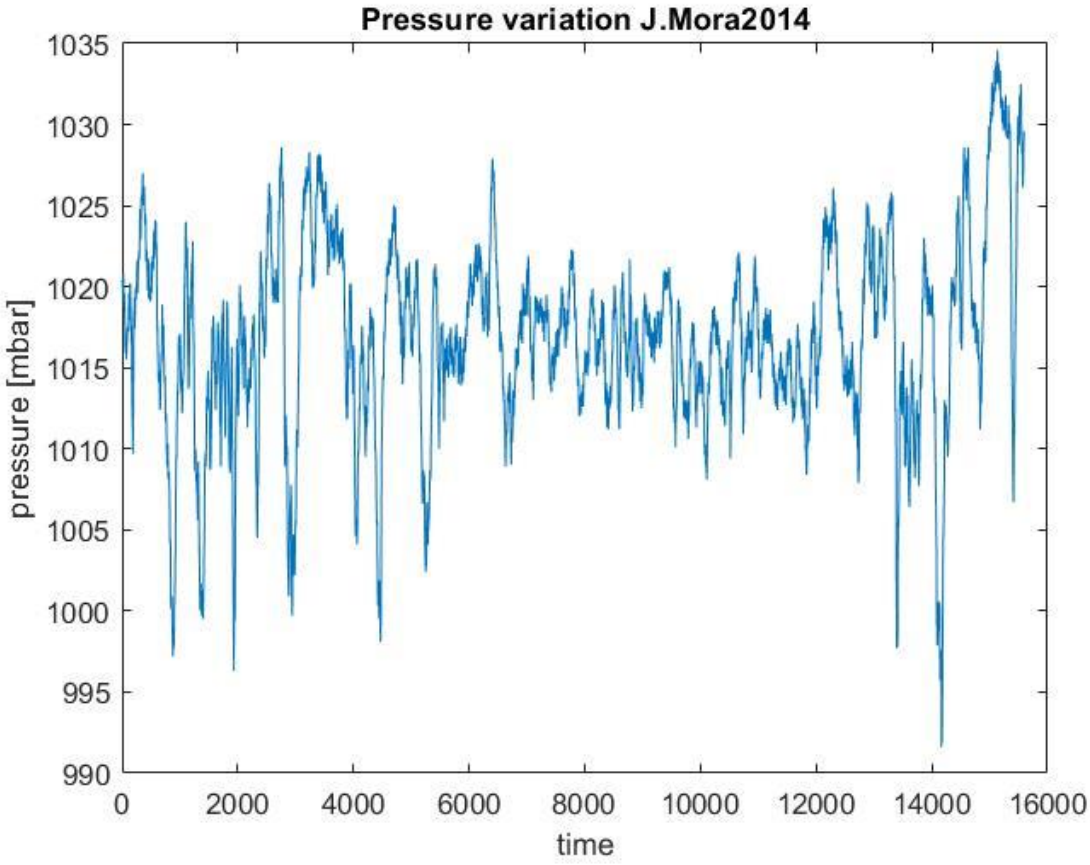


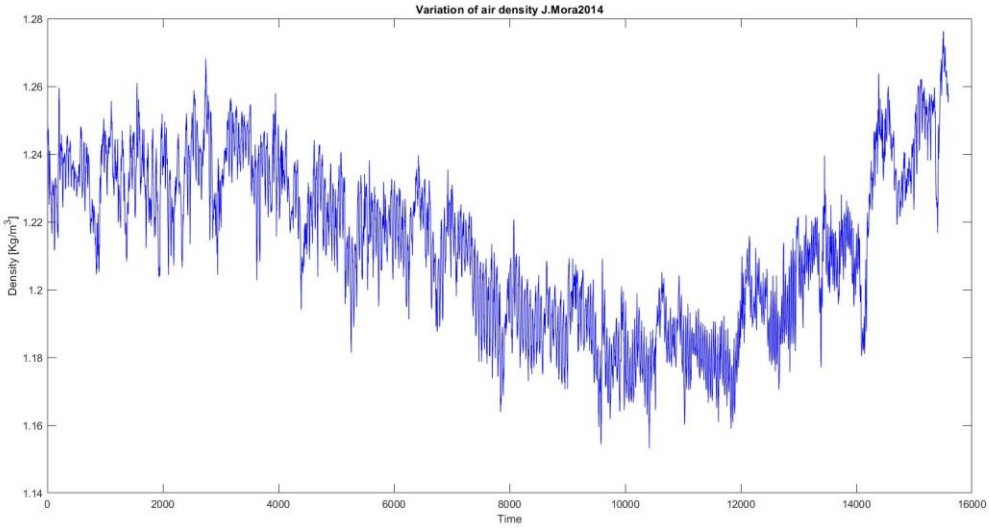


| | |
|---|---|
| Maximum Density | 1.2763 [kg/m^3] |
| Minimum Density | 1.1532[kg/m^3] |
| **Mean Density** | **1.2132**[kg/m^3] |

**Comments**
The air density follows the reverse trend of the temperature, is higher in winter and lower in summer, the annual average is kept almost constant every year, we will consider the constant density and equal to the annual average for calculations of power. Using the average air density value for energy calculation, underestimates the value in winter and overestimates in summer. However, given the small variation in density from the minimum value to the maximum value and given that the power of the wind depends mainly on the value of the cube of the wind speed, this error is negligible

### 6.3.2 Area swept by the blades.

To calculate the area swept by the blades we consider the normal surface with respect to the wind direction, considered uniform in intensity and direction with respect to all 4 turbines. The part of the surface in which the spacecraft is present is neglected in the absence of data.
There will therefore be an overestimation of the actual area. to calculate the area we will use the formula:

$$A = 4\pi \left(\frac{d}{2}\right) \text{^} 2 = 10936\ [m^3]$$

### 6.3.3 Wind speed cube

To calculate the velocity cube values that pass through the turbines, the formulas (9) and (10) are combined to extrapolate the speeds at the height where the turbines operate, starting from the velocities measured by the stations, and then elevating them to the cube.

## 6.4 Power curve and power coefficient.

To calculate the power curve, we refer to the data of the manufacturer, which consider different values of power generated at different wind speeds, taking into consideration a single wind turbine.
Obviously, the turbine produces power when the wind speed exceeds the cut-in speed up to the cut-out speed. The graphic can be divided into 3 main sections.
The first in which the control of the rotation speed of the blades intervenes to approach the maximum Cp, in which theoretically the power generated rises with the cube of the wind speed. The second when the electric power produced reaches the nominal value and the pich control intervenes on the blades, so as to produce a constant power equal to the nominal power up to the limit value of the cut-out speed in which the turbine no longer produces power.
The third is a transition zone between the other two parts, in which the turbine uses a constant number of revolutions and decreases the power coefficient with the increase of the undisturbed wind speed, in order to gradually reach the nominal power and without creating a net discontinuity between the two zones, provided by the theoretical power curve, for intervene to prevent the machine from breaking.

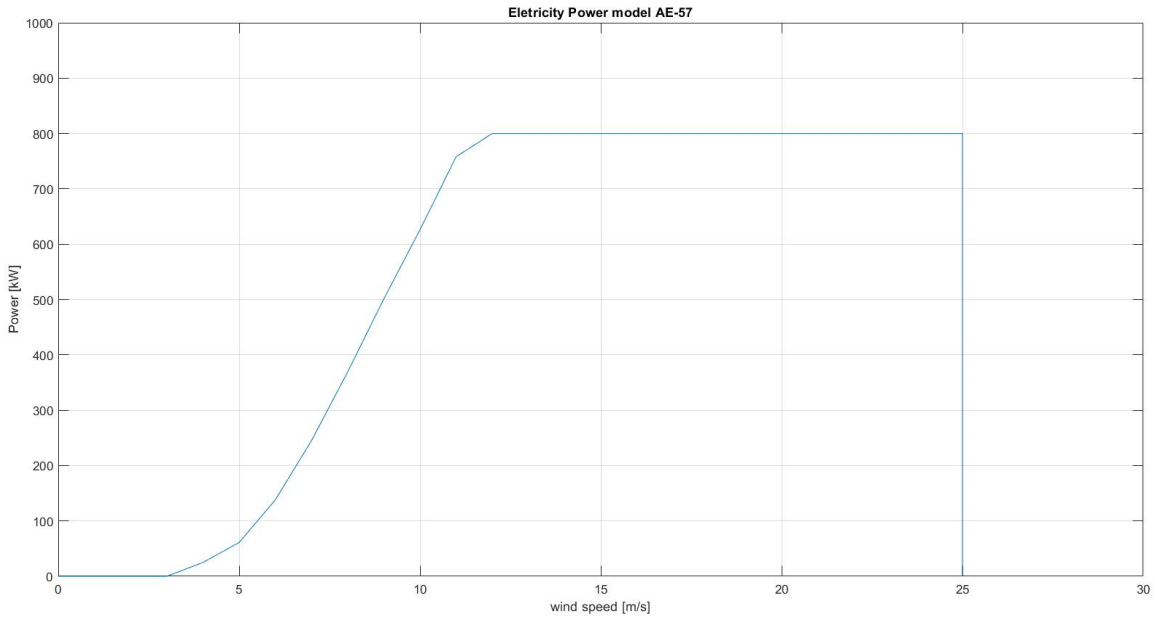


The curve of the power coefficient as a function of the wind speed was obtained with the formula (58). The power curve at the varius speeds was considered as the reference power and the undisturbed wind power was calculated for the same speeds with the formula (57). to calculate the mechanical power converted by the turbine blades, reference will be made to each wind speed extrapolated and to the wind power correlated there to which will then be multiplied by the power coefficient of the machine relative to the same speed, with the formula (58). the values of the power coefficient relative to each extrapolated speed are

then obtained by linear interpolation between the two nearest values available.

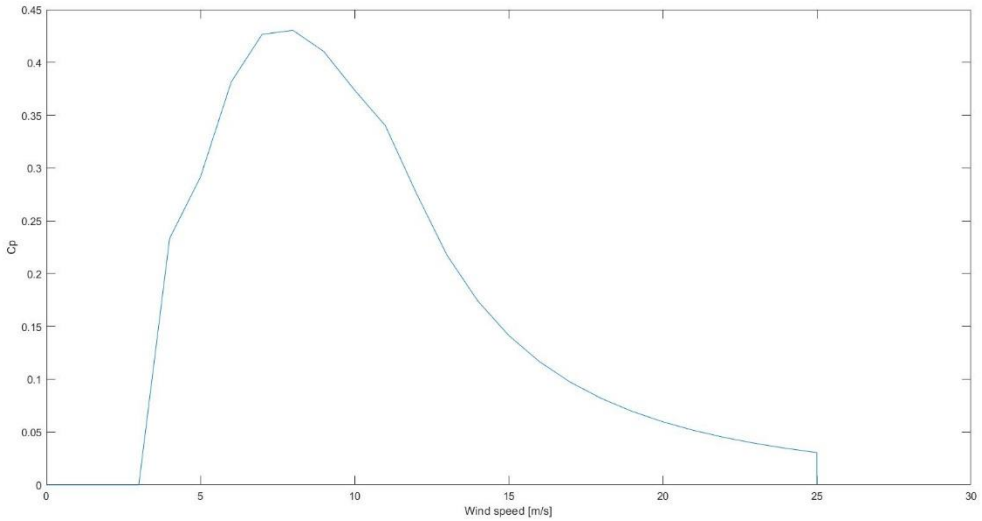


As can be seen from the graph, the power coefficient in the first part, where it operates at variable rotor speed to maximize the energy produced, grows very rapidly as the wind speed increases. However, it does not reach the maximum value in an instantaneous manner as provided for by the optimal theoretical model.
The value of the power coefficient is obviously always lower than the value of the betz theory.
Its maximum value does not correspond to the design speed of the blades, but at a lower wind speed. This can be explained by the fact that for the design wind speed of the blades 11[m/s], as seen in the power graph, it is exactly inside the transition zone to reach the nominal power, so there is a drop in the power coefficient.
Finally, we see that in the last part, when the pich control intervenes to keep the power constant at the nominal value, the power coefficient describes as the wind speed increases, until it is canceled due to the cut-out speed.

## 6.5 Electicity energy production and capacity factor

The total electric energy measurements produced by the plant divided into each hour are available. The monthly and annual energies from 2009 to 2014 will be calculated. Everything will be graphed and the annual average energy for each month will be plotted.

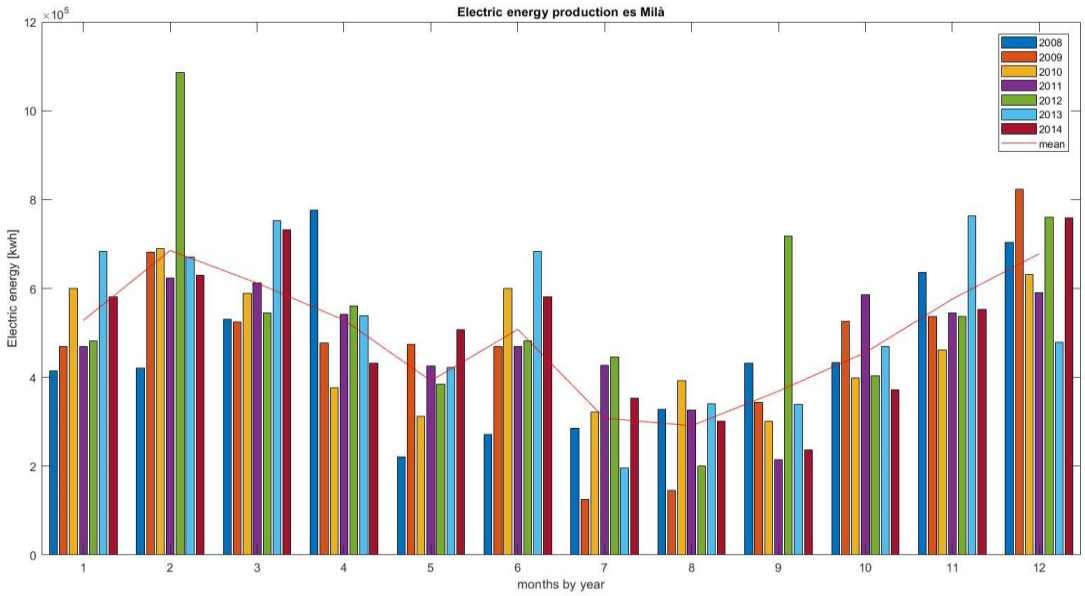


It is noted that the energy produced also varies a lot from year to year, as the wind is strongly intermittent. Note that the months when more energy is produced are winter, because the wind is faster and the air density is higher. From August to December, the average monthly energy produced grows lineary. Another very important data for a wind farm is the capacity factor, defined as the ratio between the annual energy actually produced and the one that would have been produced if the turbines had always operated under nominal conditions.

**Electric energy production es Milà [kWh]**

| **Month** | **2008** | **2009** | **2010** | **2011** | **2012** | **2013** | **2014** |
|---|---|---|---|---|---|---|---|
| Gennuary | 414922 | 468979 | 599368 | 468960 | 481557 | 683045 | 581067 |
| February | 419958 | 681402 | 689221 | 622947 | 1085474 | 669991 | 629562 |
| March | 530165 | 524552 | 588348 | 613034 | 544596 | 751841 | 732099 |
| April | 776378 | 476876 | 376748 | 541119 | 561307 | 538631 | 431287 |
| May | 221307 | 473718 | 312217 | 425414 | 384007 | 422476 | 506839 |
| June | 271914 | 468979 | 599368 | 468960 | 481557 | 683045 | 581067 |
| July | 285629 | 124869 | 321499 | 427670 | 446168 | 196045 | 353511 |
| August | 327937 | 145914 | 393148 | 326275 | 200329 | 341117 | 301622 |
| September | 431255 | 343742 | 300423 | 214206 | 717388 | 339159 | 236044 |
| October | 433830 | 526751 | 398824 | 586548 | 403514 | 468798 | 371446 |
| November | 635916 | 537815 | 461300 | 545139 | 537038 | 763682 | 552189 |
| December | 703144 | 822807 | 631827 | 590819 | 759916 | 479467 | 758724 |
| **Total year** | **5452355** | **5507421** | **5347948** | **5676918** | **6457712** | **6245630** | **5791752** |

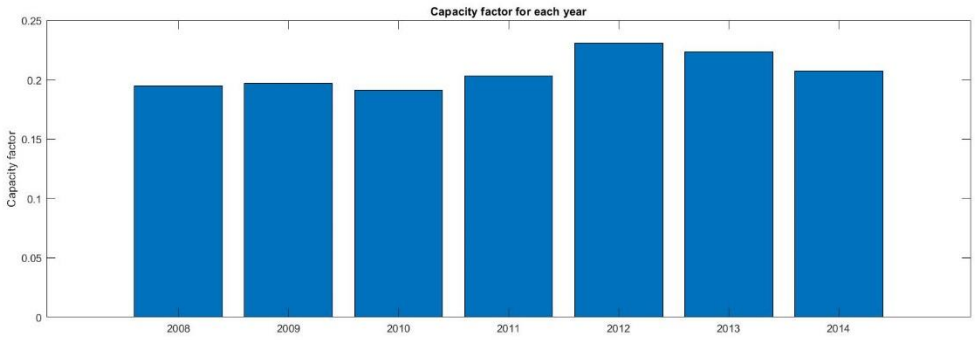


| Year | 2008 | 209 | 2010 | 2011 | 2012 | 2013 | 2014 |
|---|---|---|---|---|---|---|---|
| Capacity factor | 0,195 | 0,197 | 0,191 | 0,203 | 0,231 | 0,223 | 0,207 |

The values of the capacity factor show that on average, the energy produced in one year is approximately equal to 20% of the nominal value. it is a pretty good value even if you can also get to double in other locations. These data show how it is difficult to convert wind energy efficiently both for physical limits and for its great variability in terms of speed.

## 6.6 Theoretical energy and effective energy production

The theoretical energy produced annually is evaluated starting from the previous analyzes using the model in point 6. Moreover, the ratio of the electricity produced for each year is evaluated considering in the missing data for wind speed measurements an even wind speed equal to 0 [m/s].

The theoretically producible energy is expected to be always greater than that actually produced for the following reasons:

1. In the calculation of the theoretical energy it is assumed that all 4 turbines, are always working because it is known the total electricity produced by the plant and not the single turbines.
2. It is assumed that there is never interference between the turbines themselves, this hypothesis is true only when the wind direction coincides with the directions of maximum wind energy, found in the wind rose analysis. But when the wind direction aligns, for example, with two turbines, the upstream turbine reduces the wind energy made available for that downstream, consequently reducing the total energy produced.
3. Using the power coefficient curve obtained from the machine data, it is assumed that the undisturbed wind direction is purely axial and always coincides with the axis direction of all the turbines. But when the wind direction also has a tangential component (which is very frequent for the breeze phenomenon), there is a reduction in the apparent area swept by the blades and a reduction in the power coefficient.
4. in the calculation of the theoretical energy we consider only the mechanical energy available at the rotor, we do not consider therefore the conversion to electrical energy and the losses of the electric generator

**Result**

| **Year** | **2009** | **2010** | **2011** | **2012** | **2013** | **2014** |
|---|---|---|---|---|---|---|
| **Energy ratio** | **1,28** | **0,99** | **1,07** | **1,15** | **1,05** | **0,73** |

as can be seen from the first results in some cases the energy actually produced is even higher than that theoretically producible. This is due to the fact that it was chosen to set the wind speed to 0 during the hours when the measurements are not available, when the wind power plant actually produced energy. In order to have a more likely estimate, the values set equal to zero previously has been replaced by the values of the annual average velocity measured for each year extrapolated to the height of the turbines.

**Numer of hours (days) that the measurements are not avaiable**

| **Year** | **2009** | **2010** | **2011** | **2012** | **2013** | **2014** |
|---|---|---|---|---|---|---|
| hours (days) | 491 (20.4) | 957 (39,9) | 140.5 (5.9) | 246.5 (10.3) | 672.5 (28) | 2054.5 (85,6) |

**Theoretical energy production [kWh]**

| **Year** | **2009** | **2010** | **2011** | **2012** | **2013** | **2014** |
|---|---|---|---|---|---|---|
| | **7433603** | **5556022** | **6227546** | **7661282** | **7261072** | **6420655** |

**Energy ratio**

| Year | 2009 | 2010 | 2011 | 2012 | 2013 | 2014 |
|---|---|---|---|---|---|---|
| Energy ratio | 1,34 | 1,04 | 1,10 | 1,18 | 1,16 | 1,11 |

**Comments**

In 2009 the theoretical energy produced exceeds the effective energy of 34%. The figure is very different from those of other years. This is probably because in the year 2009 at least one of the 4 turbines were not working for a few times, also if the wind speed measurements show that were a particularly windy year. If in other years a continuous operation of all 4 turbines is assumed, we see that the theoretical model overestimates the energy produced by 4% to 18% and the overestimation is higher in the windiest years.

# 7 Conclusions

The analysis of this thesis highlights how to try to describe the correlation between the meteorological data and the behavior of a wind farm it is necessary to create an extremely simplified model with respect to reality. Many hypotheses have been made upstream, some are often verified while others are less, but almost always are necessary assumptions related to the fact that the wind is highly variable and difficult to predict, in terms of intensity and direction. The aim of this thesis is also to show the critical aspects of wind analysis and be a starting point for further analysis.

## Reference


1. Giorgio Pavesi: Wind energy systems (notes for students), dipartimento di ingegneria industriale, Padova, 2013.
2. Wind energy handbook, Second edition, Tony Burton, Nick Jenkins, David Sharpe and Ervin Bossanyi. © 2011 John Wiley & Sons, Ltd. Published 2011 by John Wiley & Sons, Ltd. ISBN: 978-0-470-69975-1
3. Burr, I. W.: Applied Statistical Methods, Academic Press, New York, 1974.
4. Climatography of the United States, Series 82: Decennial Census of the United States Climate, "Summary of Hourly Observations, 1951-1960" (Table B). Cole, F. W.: Introduction to Meteorology, Wiley, New York, 1970. Corotis, R. B.: Stochastic Modelling of Site Wind Characteristics, ERDA Report RLO/2342-77/2, September 1977.
5. Corotis, R. B., A. B. Sigl, and J. Klein: "Probability Models of Wind Velocity Magnitude and Persistence," Solar Energy, Vol. 20, No. 6, 1978, pp. 483-493. Corotis, R. B.: Statistic Models for Wind Characteristics at Potential Wind Energy Conversion Sites, DOE Report DOE/ET/20283-1, January 1979.
6. Donn, W. L.: Meteorology, McGraw-Hill, New York, 1965.
7. Elliott, D. L.: Synthesis of National Wind Energy Assessments, Pacific Northwest Laboratory, Richland, Wash., Report NTIS BNWL-2220 WIND-5, 1977.
8. Golding, E.: The Generation of Electricity by Wind Power, Halsted Press, New York, 1976. Gumbel, E. J., Statistics of Extremes, Columbia University Press, New York, 1958.
9. Henry, David H. and Gary L. Johnson: "Distributions of Daily Extreme Winds and Wind Turbine Operation," IEEE Transactions on Power Apparatus and Systems, Vol. EC-1, No. 2, June, 1986, pp. 125-130.
10. Justus, C. G.: Winds and Wind System Performance, Franklin Institute Press, Philadelphia, 1978.
11. Justus, C. G., K. Mani, and A. Mikhail: Interannual and Month-to-Month Variations of Wind Speed, DOE Report RLO-2439-78/2, April 1978.
12. Liu, H.: "Matching WECS Survivability with Severe Wind Characteristics: A Rational Approach," Wind and Solar Energy Conference, Kansas City, Mo., April 5-7, 1982.
13. Marrs RW Marwitz J (1977) Locating areas of high wind energy potential by remote observation of eolian geomorphology and topography. Third Wind Energy workshop (CONF 770921), Washington DC, pp307- 320
14. Odette, D. R.: A Survey of the Wind Energy Potential of Kansas, M.S. thesis, Electrical Engineering Department, Kansas State University, Manhattan, Kans., 1976.
15. Panofsky, H. A.: "Wind Structure in Strong Winds below 150 m," Wind Engineering, Vol. 1, No. 2, 1977, pp. 91-103.
16. Pasquill, F.: Atmospheric Diffusion, 2nd ed., Halsted Press, New York, 1974.
17. Putnam, P.C.: Power from the Wind, Van Nostrand, New York, 1948.
18. Riehl, H.: Introduction to the Atmosphere, McGraw- Hill, New York, 1965.
19. Simiu, E., M. J. Changery, and J. J. Filliben, Extreme Wind Speeds at 129 Stations in the Contiguous United States, NBS Building Science Series 118, National Bureau of Standards, Washington, D. C., March 1979.
20. Spera, D. A., and T. R. Richards: "Modified Power Law Equations for Vertical Wind Profiles," Conference and Workshop on Wind Energy Characteristics and Wind Energy Sitting 1979, Portland, Oreg., June 1979, Pacific Northwest Laboratory, Battelle Memorial Institute, Report PNL-3214.

21. Cavallini, Energia Eolica Appunti per il corso di Energie Rinnovabili', Padova.

Link

https://windeurope.org
http://dgener.caib.es/www/pie/energies_renovables/es_mila_1.html
http://www.riemenorca.org/Contingut.aspx?IdPub=8836&menu=Energia
https://es.wikipedia.org/wiki/Parque_e%C3%B3lico_de_Es_Mil%C3%A0
https://www.en.wind-turbine-models.com/turbines/
https://www.thewindpower.net/turbine_en_52_made_ae-59.php